

FACILITY FORM 602  
N66-20892  
(ACCESSION NUMBER)  
109  
(PAGES)  
CR 71163  
(NASA CR OR TMX OR AD NUMBER)

(THRU)  
1  
(CODE)  
14  
(CATEGORY)

FINAL REPORT  
FOR

NASA CR 71163

AN EXPERIMENTAL EFFORT TO IMPROVE THE  
NIMBUS HIGH RESOLUTION INFRARED RADIOMETER

VOLUME I OF TWO VOLUMES

(1 May 1964 - 15 February 1965)

Contract No. : NAS 5-3683

Work Order: 65-2-4/65-1-65

Prepared by

ITT Industrial Laboratories  
Fort Wayne, Indiana

For

National Aeronautics & Space Administration  
Aeronomy and Meteorology Branch  
Goddard Space Flight Center  
Greenbelt, Maryland

GPO PRICE \$ \_\_\_\_\_

CFSTI PRICE(S) \$ \_\_\_\_\_

Hard copy (HC) \$ 4.00

Microfiche (MF) .75

FINAL REPORT  
FOR  
AN EXPERIMENTAL EFFORT TO IMPROVE THE  
NIMBUS HIGH RESOLUTION INFRARED RADIOMETER

(1 May 1964 - 15 February 1965)

Contract No. : NAS 5-3683

Work Order: 65-2-4/65-1-65

Prepared by

ITT Industrial Laboratories  
Fort Wayne, Indiana

For

National Aeronautics & Space Administration  
Aeronomy and Meteorology Branch  
Goddard Space Flight Center  
Greenbelt, Maryland

Contributors

W. H. Wallschlaeger, P. C. Murray,  
P. R. Sargent, R. V. Annable

Approved by



W. H. Wallschlaeger,  
Project Manager



K. L. DeBrosse, Manager  
Space & Physical Sciences Dept.

## ABSTRACT

Modifications have been made to the Nimbus HRIR Prototype No. 2 on Contract NAS5-3683, Work Orders 65-2-4 and 65-1-65. This report will explain how these modifications were accomplished and the experimental results caused thereby.

The effort included under electronics changes are:

1. Design and incorporation of a lower noise preamplifier.
2. Electronic generation of a compensating signal for chopper emission.
3. Full time telemetry.
4. Temperature stabilization of electronics for ambient temperatures from -30 degrees C to +55 degrees C.
5. Temperature control of detector above -95 degrees C.
6. Generation of calibrated step voltage of 0 to 6 volts in 1 volt steps at output during 1/3 of housing scan time.
7. Incorporation of 30 rpm scan rate with bandwidth change to 184 cps.

Other changes which were made to improve the detector cooling were:

1. Tests to show the merit of using a fiberglass instead of a KIA magnesium secondary casting.
2. Tests to show the feasibility of the use of titanium alloy support wires for the cooling patch support.
3. Cooling patch and cell holder to be made of magnesium.

In addition to these, tests were to be made to determine if the radiometer met Nimbus Environmental Specifications. All the modifications covered by the work statement were incorporated into prototype No. 2.

Laboratory tests on the bench and within an environmental space chamber were performed on this unit to establish the relative success of the changes and to indicate possible problem areas. Tests on the bench indicated an improvement in the noise figure of the preamplifier from an average value of 3.5 db for the former

design to an average of less than 1 db for the new design. However, tests on the entire subsystem showed no visible improvement in the noise level. These results show that the system is most certainly detector noise limited now and possibly was before.

There were problems involved in the circuit design for the chopper emission compensation signal. A design was finally arrived at which worked for this unit. By putting all telemetry points on the full time power (regulated) the full time telemetry capability was accomplished.

Electronic amplifiers were stabilized to  $\pm 1$  db gain variation over the specified temperature range. The voltage regulators were stabilized to  $\pm 1$  percent over the same range. The calibrated staircase step voltage is multiplexed with the output during the housing scan. It should be mentioned that the electronics did not reach the low temperatures expected and a lower limit of  $-5$  degrees C instead of  $-30$  degrees C would probably be adequate.

To achieve the desired 30 rpm scan rate, the gear train was redesigned and new gears procured from a different manufacturer. The gear assemblies did not stand up under vibration and were modified to do so.

Environmental tests on the fiberglass casting and the support rings with titanium wire proved the reliability of this design. Radiant cooling tests showed that these design changes did indeed improve the cooling capabilities of this unit.

The recommendations which ITTIL engineering would make after analyzing these modifications and the test results are:

1. Due to its inherently better stability and relatively better insensitivity to radiation, the field effect preamplifier should be part of any new design.
2. The electronic offset generation as used in this unit has some deficiencies as yet. We have, however, designed a quadrature filter for use with this circuit which should eliminate them.
3. The fiberglass secondary casting and the titanium support wires, having proven their worth, should be incorporated into new designs.

## TABLE OF CONTENTS

	Page
1.0 INTRODUCTION -----	1
2.0 ELECTRONICS MODIFICATIONS -----	3
2.1 Low Noise Preamplifier -----	6
2.2 Electronic Offset -----	8
2.2.1 Variable Gain Amplifier -----	10
2.2.2 AGC Control Circuit -----	13
2.3 Full-Time Telemetry -----	13
2.4 Cell Temperature Control -----	16
2.5 Calibration Step Voltage -----	18
2.5.1 Time Positioning -----	18
2.5.2 Step Voltage Generation -----	21
2.5.3 Multiplexing -----	24
2.6 Scan Rate and Bandwidth Changes -----	24
2.6.1 Gear Changes -----	24
2.6.2 Mirror Magnetic Pickup -----	28
2.6.3 Bandwidth Changes -----	28
3.0 DETECTOR COOLING MODIFICATIONS -----	31
3.1 Fiberglass Electronic Casting -----	31
3.2 Titanium Alloy Support Wires -----	32
3.3 Magnesium Patch -----	37
4.0 TESTS -----	43
4.1 Cell Cooling Tests -----	43
4.2 Field of View Measurements -----	46
4.3 Humidity -----	51
4.4 Vibration -----	51
4.5 Acceleration -----	77
4.6 Radiometric Calibrations -----	77
5.0 NEW TECHNOLOGY -----	89
5.1 Epoxy Cooling Patch Support Rings -----	89
5.2 Detector Temperature Control -----	89
5.3 Electronic Offset -----	89

## LIST OF ILLUSTRATIONS

Figure		Page
1	Functional Block Diagram of Modified Prototype 2 Radiometer -----	5
2	Low Noise Preamplifier Circuit -----	7
3	HRIR Radiometer Noise Figure Versus Source Resistance Low-Noise FET Preamp.-----	9
4	Block Diagram - Electronic Offset -----	11
5	Variable Gain Amplifier -----	12
6	AGC Control Circuit -----	14
7	-20V F/T Regulator -----	15
8	Original Cell Control Circuit -----	17
9	Improved Cell Control Circuit -----	17
10	Typical Cell Temperature Cycling at 0°C -----	19
11	Block Diagram - Staircase Voltage Generator -----	20
12	Staircase Generator Circuit-----	22
13	Transfer Gate Circuit-----	22
14	Oscilloscope Trace - Staircase Voltage -----	25
15	Visicorder Trace Showing Staircase Voltage -----	26
16	Scan Drive System for 30 RPM-----	27
17	Low Pass Filter Circuit -----	29
18	Low-Pass Filter Response 184 cps -----	30
19	Synthane Casting Assembly -----	33
20	Radiation Cooler Assembly -----	34
21	New Patch Suspension System -----	35
22	Alternate Patch Suspension Assembly -----	38
23	Suspension System Test Configuration -----	39
24	Cell Cooling Versus Time HRIR Radiometer Model P-2M/2 -----	47
25	Field of View Plot -----	50

## LIST OF TABLES

Table 1	Capacitor Temperature Stability Comparison -----	23
Table 2	Properties of Wire Types -----	36
Table 3	Vibration Test of Suspension Range -----	40
Table 4	Cooling Run - August 17, 1964 -----	44
Table 5	Colling Run - August 19, 1964 -----	45
Table 6	Comparison of Cell Cooling Capabilities -----	48
Table 7	-----	49

## 1.0 INTRODUCTION

The International Telephone and Telegraph Industrial Laboratories (ITTIL) is pleased to submit this final report on the modification of the prototype 2 HRIR. These modifications were made as an experimental effort to improve the HRIR sensitivity and detector cell cooling. Later additions to the program were the inclusion of a calibration step voltage, a change in scanning rate, and a change in information bandwidth.

The radiometer as used on Nimbus A had certain deficiencies. Among these were:

1. Inadequate detector cooling with a warm satellite (i. e. satellite temperature above 25 degrees C)
2. Possible lack of reliability associated with the light bulb generating the chopper compensation signal
3. Possible noise inputs from the preamplifier

The modification program was intended to determine the possibilities of eliminating such deficiencies. The program was set up so that parallel efforts were made on mechanical and electrical changes. Following a period of design, the various components were assembled at a subsystem level, tested, redesigned, retested and assembled finally into the modified HRIR. The testing was used to determine temperature and vibration effects as well as to establish the effectiveness of the design intent.

After assembly, the HRIR was put through a series of space chamber tests to determine the effects of the modifications on the over-all system. The radiometer was then tested to the Nimbus B environmental specifications. Some problems were experienced during vibration with the new gearing used to effect the scan rate change.

The work and tests performed indicated the following:

1. The preamplifier noise, while improved, did not result in any significant improvement in sensitivity. The detector noise, due to a predominance in current noise, apparently makes the system detector noise limited with either preamplifier. However, the new preamplifier is more resistant to radiation and drift.
2. Chopper compensation was achieved by entirely electronic means. Several different methods were attempted and the final design still had problems due to quadrature nulls.

3. The cell cooling was improved to the extent that temperatures up to 40 degrees C at Reference A could be tolerated. Previously, the maximum tolerable temperature for Reference A at which cell cooling was sufficient was about 15 degrees C.

This modification has provided much information leading to design improvements as well as reliability improvements. The following sections tell a more complete story of the accomplishments of the program. Electronic modifications are covered first, followed by an explanation of the detector cooling changes. Next the results of performance and environmental tests are related and the radiometric calibration of the complete instrument is given. New technology developed on the program is described in Section 3.0, and supporting information is contained in the appendixes.



## **2.0 ELECTRONICS MODIFICATIONS**

The electronics modifications as called out by the work statement are:

1. Low Noise FET Preamplifier
2. Electronic Offset
3. Full Time Telemetry
4. Temperature Stabilization
5. Cell Temperature Control
6. Calibration Step Voltage
7. Bandwidth Changes

The additional circuitry associated with these changes and additions required the rearrangement of the printed circuit boards and modules. The packaging is still made up of three boards and two modules but now arranged as follows:

### **Board No. 1**

1. Video Amplifier
2. Log Amplifier
3. AGC Amplifier

### **Board No. 2**

1. Reference Signal Generator
2. Demodulator
3. Output Amplifier
4. AGC Control
5. -20 volt Regulator for D/N Power

### **Board No. 3**

1. Marker Pulse Generator

2. -20 volt Telemetry
3. Video TM
4. Staircase Voltage Generator

Module No. 1

1. Preamplifier
2. Detector Cell Temperature TM and Control

Module No. 2

1. -20 Volt Regulator for Full Time Power
2. Motor Low Pass Filter
3. Temperature TM

The new printed circuit boards are made of FR-45 material (Formica Corporation) which has low leakage qualities. The circuitry is gold plated on all boards and modules. The electronics density in the available space has now reached the point of new saturation. Additional modifications will require expanded limits to the electronics volume.

A block diagram of the modified prototype 2 radiometer is shown in Figure I. Radiation reflected from the scan mirror is focused by the telescope onto the chopper, which modulates the radiant signal. The relay optic filters the radiation to the 3.4 to 4.2 micron band and refocuses it onto the detector. The detector temperature is regulated by an improved cell temperature control (Section 2.4). The video electrical signal from the detector is amplified by the low-noise preamplifier (Section 2.1) and the video amplifier. The video and electronic offset (Section 2.2) signals are then fed to the log amplifier and the corrected video amplified and synchronously demodulated by a reference signal from the chopper pickup. The output of the demodulator is passed through a low-pass filter to produce the output video. The cutoff frequency of the output filter and rotational speed of the scan mirror have been changed to 184 cps and 30 rpm, respectively (Section 2.6). Synchronization is provided by the marker output which originates from the mirror pickup (Section 2.6.2).

The output video is integrated to give a telemetry output that is one of ten full-time telemetry outputs (Section 2.3). The output video is also fed to the AGC control to regulate the injection of the electronic offset signal (Section 2.2). Finally, the output video is gated with the calibration step voltage (Section 2.5) to produce the radiometer output signal.

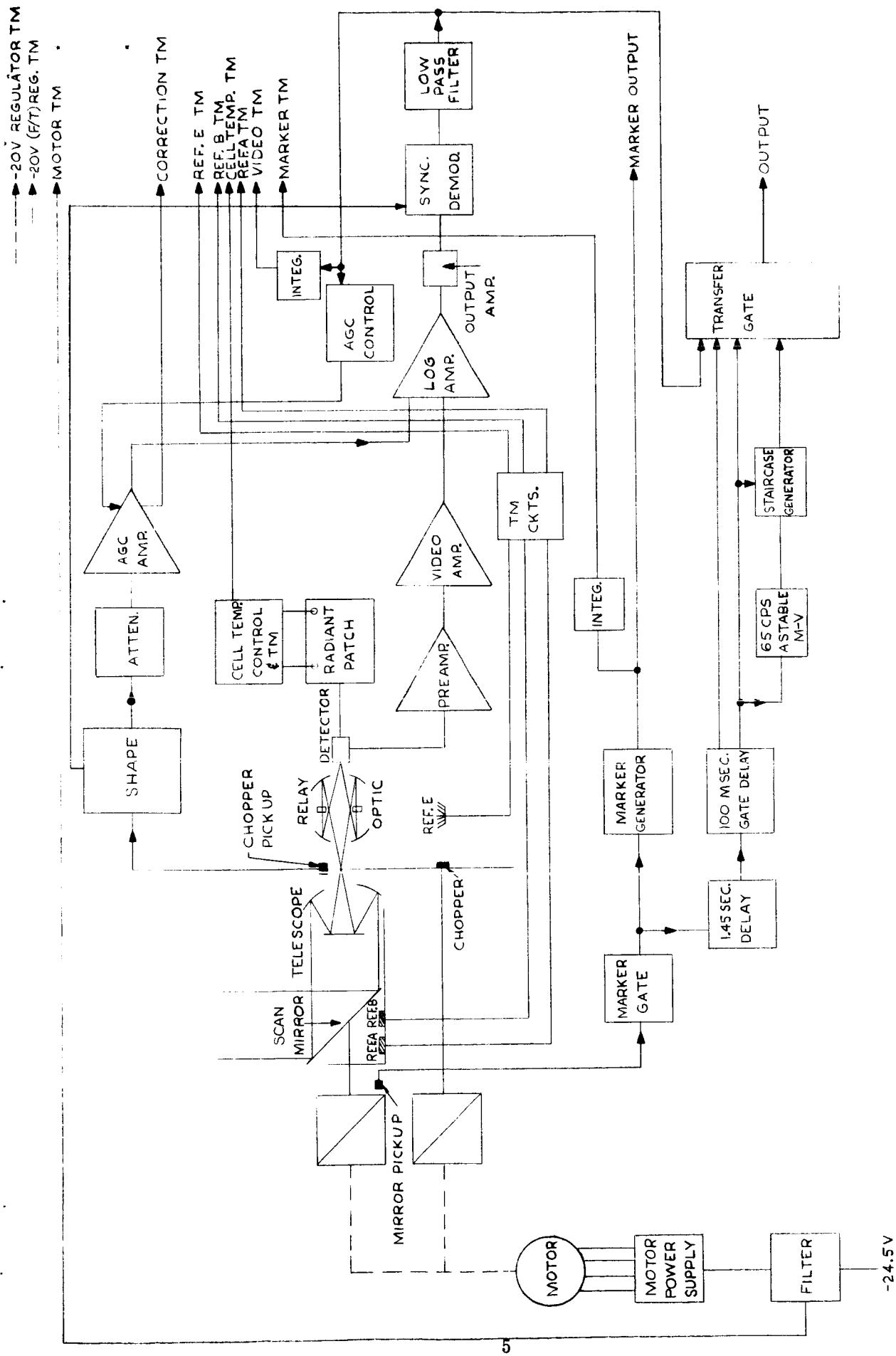


Figure 1 Functional Block Diagram of Modified Prototype 2 Radiometer

## 2.1 Low Noise Preamplifier

The object of this modification was to provide a preamplifier which would add less noise to the system and thereby produce a system which is more nearly detector noise limited. The old preamplifier had an average noise figure of about 3.5 db. The noise figure is a quality factor for an amplifier expressing the amount of noise added by the amplifier with respect to the white (Johnson) noise of the generator resistance. This may be expressed by the equation

$$NF (db) = 10 \log_{10} \frac{P_A + P_R}{P_R}$$

where  $P_A$  = noise power generated by the amplifier

$P_R$  = white noise power generated by the generator resistance.

It can be seen that if  $P_A = 0$ , the noise figure = 0 db and if  $P_A = P_R$ , the noise figure = 3 db.

The generator resistance seen by the HRIR preamplifier is the parallel combination of the cell and the load resistances. The load resistor is 3 megohms while the cell resistance is variable from about 2 megohms to 20 megohms. The generator resistance is then between 1.2 megohms and 2.6 megohms. The input impedance of the preamplifier must be high enough so that loading effects do not reduce the signal level. The output impedance must be low to reduce cable capacitance effects.

The first stage is selected for noise qualities as well as high input impedance. A device which combines these qualities is the field effect transistor (FET). The 2N2500 FET guarantees a noise figure of 1 db for  $R_G = 1$  megohm,  $f = 1000$  cps,  $I_D = -1$  ma and  $V_{DS} = -5$  volts. This corresponds to the levels we are trying to achieve, so this FET was selected for the first stage. The 2N2500 also has a guaranteed maximum input capacitance of 32 pf. If the maximum capacitance is encountered, the input impedance at 1500 cps is about 3.3 megohms. The preamplifier must therefore be designed with a feedback to eliminate the capacitive effects of the input.

The preamplifier schematic is shown in Figure 2. The first stage, Q-1, is a source follower feeding into Q-2, a 2N930, operating as an emitter follower. The terminal of Q-1 connected to C-2 is the gate, the terminal connected to R-8 is the drain, and the terminal connected to R-9 is the source. The drain current ( $I_D$ ) is about -1 ma, while the drain to source voltage ( $V_{DS}$ ) is about -7 volts. The gate is dc biased from a split source resistor so that  $V_{GS} = 1.3$  volts while R-10 is returned to the emitter resistor (R-12) of Q-2. The current through R-12 is a combination of  $I_{D1}$  and  $I_{E2}$  providing a degree of temperature stability to the operating point of Q-1.

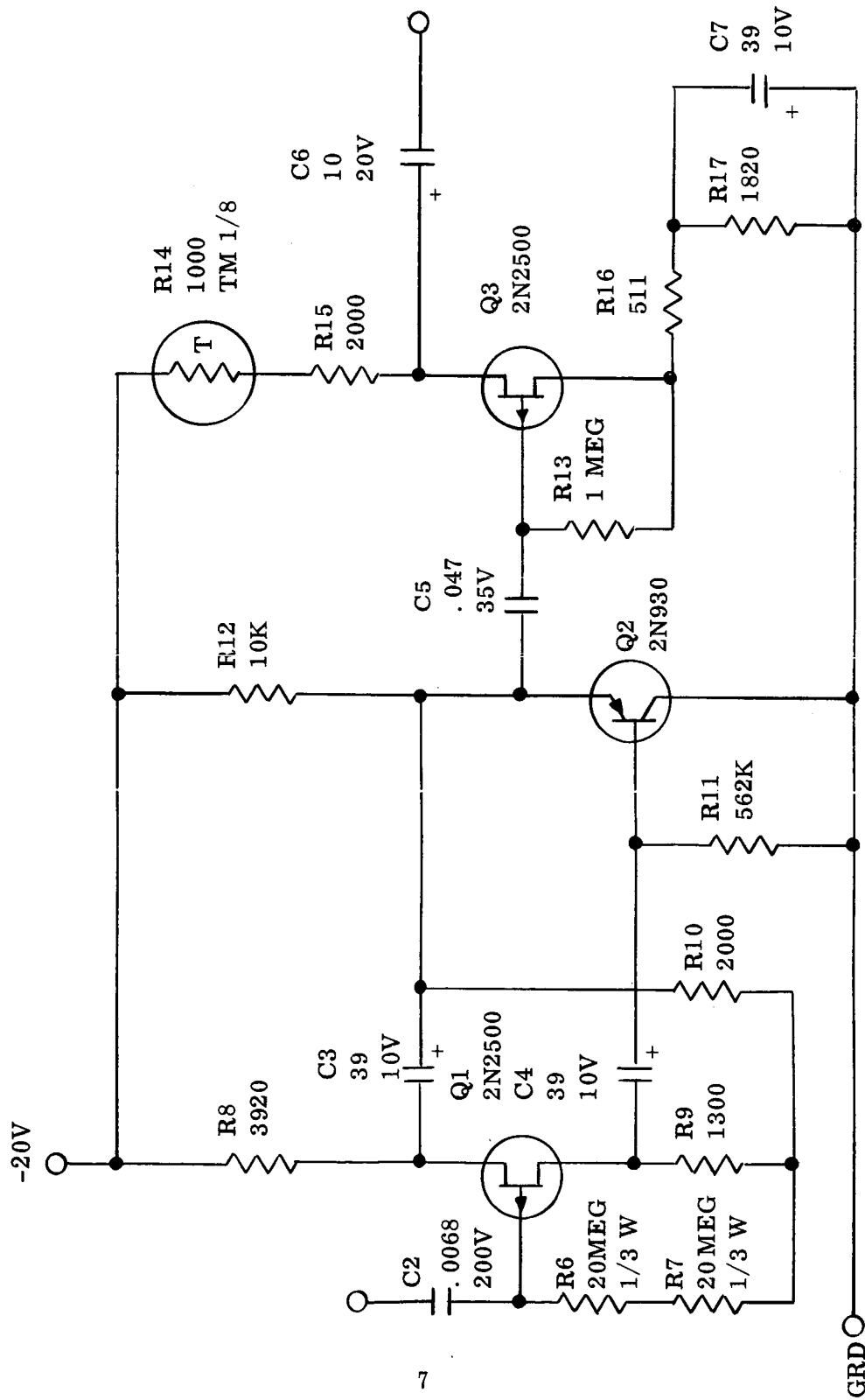


Figure 2 Low Noise Preamplifier Circuit

The method of biasing the gate with gate resistors R-6 and R-7 reduces part of the input capacitance, and bootstrapping the drain of Q-1 to the emitter of Q-2 adds to this effect. The preamplifier input impedance at 1500 cps is 90 megohms measured. Figure 3 shows that the noise figure is 1 db or less for source resistances ranging from 0.63 megohm to 10 megohms. With a generator resistance of 2.7 megohms, the preamplifier is 3 db down at 250 cps and at 16.8 kc. The response is maximum and flat within 0.2 db from 870 cps to 4.3 kc.

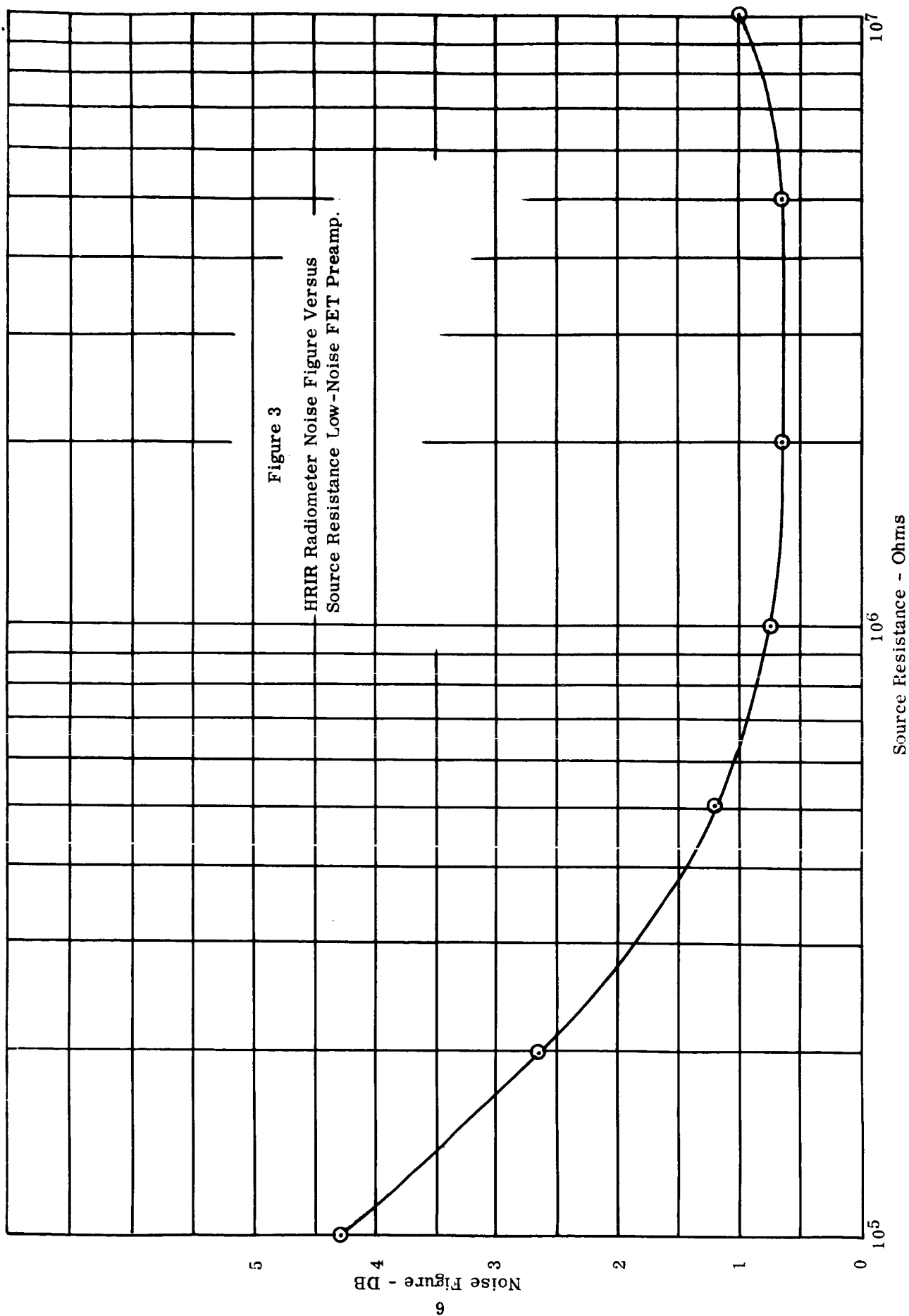
The resistor shown as R-14 is a 1000 ohm sensistor which temperature stabilizes the preamplifier. The output impedance is set by R-14 and R-15 and is 3000 ohms. This combination will, in the future, be tailor points for temperature stabilization.

## 2.2 Electronic Offset

In order to realize the full benefit of a decrease in preamplifier noise, other sources of inaccuracies in the radiometer must be kept small. The largest of these other sources is the residual signal produced when the internal (chopper) radiation signal is not accurately balanced or compensated. This problem with the HRIR is inherent in low-temperature radiometric instruments employing a rotating mechanical chopper. The chopper itself becomes a source of radiation during the "blade-closed" portion of the chopping cycle, either by its own emission or by reflecting emission from other internal sources. If the background, or target radiation is lower in magnitude, i. e. colder than the chopper disc, the resultant output from the detector cell appears as a signal 180 degrees out of phase with the normally chopped target signal. Since synchronous demodulation is used at the radiometer output, this chopper radiation causes a positive going d-c output rather than the normal negative target signal. This unwanted radiation signal has been offset in previous models by placing a collimated light beam behind the chopper so as to balance out any out-of-phase radiation. The intensity of the light beam was automatically regulated to exactly balance the chopper signal when the radiometer viewed cold space or a cold blackbody source.

The disadvantages of this method of radiation balance are threefold:

1. It is extremely difficult to physically position the light source so as to provide an exact 180 degree phase difference with the chopper signal.
2. The environmental reliability of the filamentary light bulb is not as high as would be desirable.
3. If it is desired to use a cooled filter on the face of the detector cell, this method of radiation bias would be impractical.



If an out-of-phase electronic signal could be introduced prior to the logarithmic amplifier, these three problems would be eliminated.

The original approach to electronic compensation was to remove the fundamental 1500 cps sine wave from the demodulating square wave and use this for a correction signal. The process of extracting the fundamental sine wave presented a serious phase stability problem. In the twin-T active filter, the phase shift is exactly 180 degrees only when the twin-T network is peaked precisely at  $f_0$ . Any slight shift in the incoming signal ( $f_0$ ) or a slight parameter shift in the network will cause the phase to be other than 180 degrees. The net result of this phase shift is a quadrature null at the demodulator and a reduced demodulator efficiency.

In an effort to reduce or eliminate this problem, it was decided to use the original reference signal square wave, inverted 180 degrees by an amplifier, for the correction signal. This approach worked very well at low ambient temperatures; however, at higher temperatures the third order harmonics generated in the nulling process caused considerable compression of the low level radiant signals by the log amplifier. Thus the sensitivity at higher satellite temperatures was degraded beyond acceptable limits.

The final solution to the problem uses the square wave compensation signal, but with tuned circuits in the first two stages of the log-amplifier. These circuits are stagger tuned about the 1500 cps center frequency. In this manner the undesirable third harmonic components are attenuated to the extent they no longer present a problem. Tests over the entire 0 to 50 degree C temperature range yielded good results with the maximum null signal reaching approximately 400 mv. at the output of the log amplifier. A block diagram of the complete system is shown in Figure 4.

#### 2.2.1 Variable Gain Amplifier

Following attenuation to a sufficiently low level, the reference square wave signal is fed to a controlled variable gain amplifier, shown schematically in Figure 5. The variable gain (AGC) feature is provided by utilizing the voltage variable resistance characteristic of the field-effect transistor, Q-6. As the gate to source d-c voltage is varied, the drain to source effective resistance is also varied. By using the transistor as a degenerative feedback resistor in the emitter of Q-5, the over-all gain can be controlled by varying the field-effect transistor gate voltage. Transistor Q-7 is simply a buffer amplifier between the high impedance AGC stage and the relatively low impedance operational amplifier. Variable resistor R-22 allows for setting the maximum signal level. Maximum dynamic range of the circuit using 0 to -10 volts dc gate voltage is approximately 60 db.



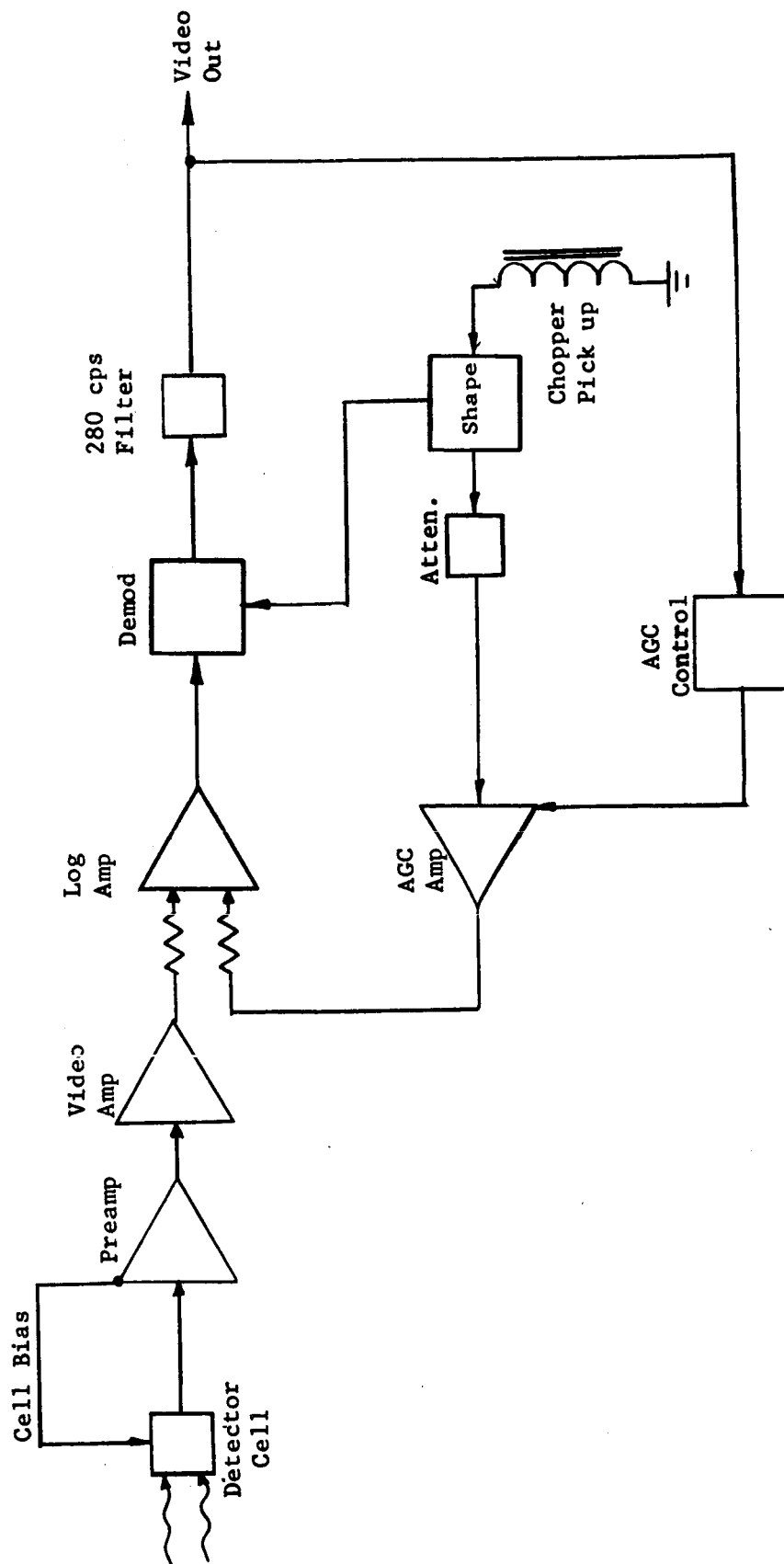


Figure 4 Block Diagram - Electronic Offset

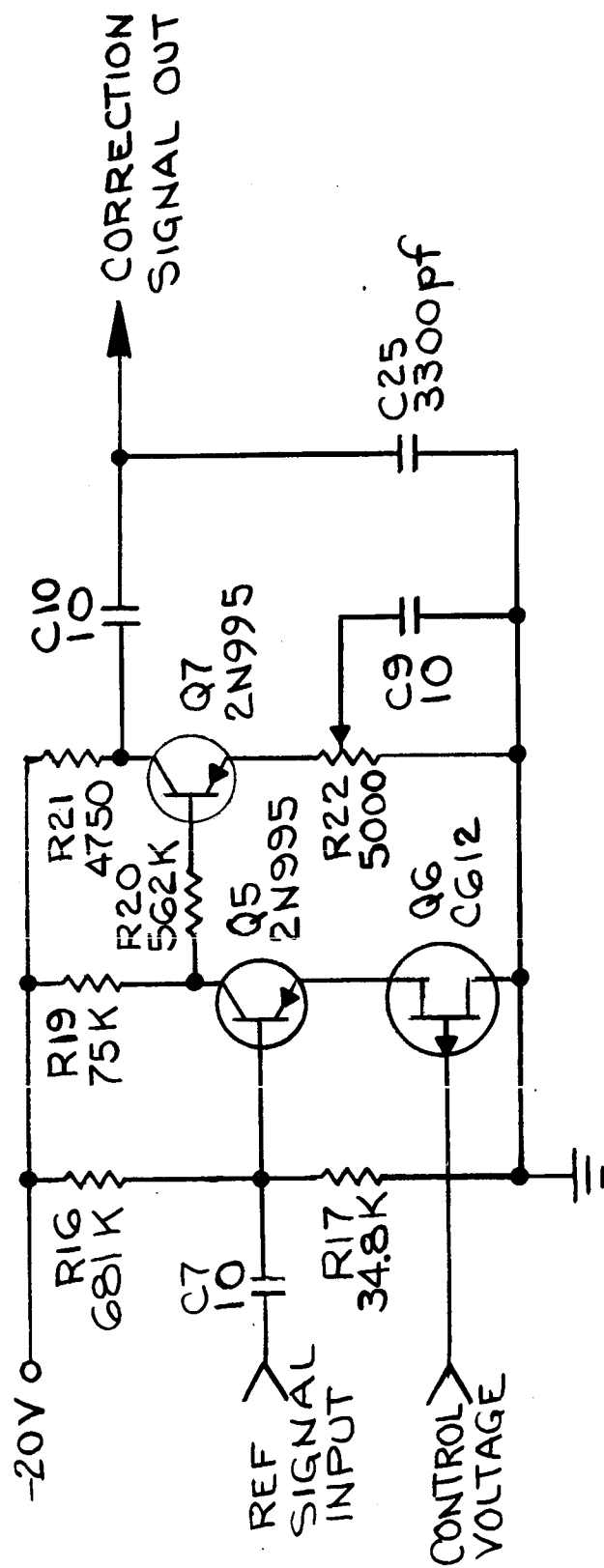


Figure 5 Variable Gain Amplifier

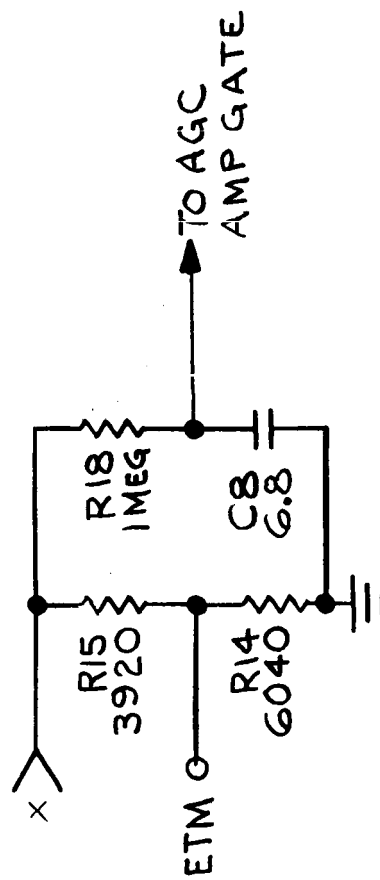
### 2.2.2 AGC Control Circuit

Control voltage for the gate of the AGC amplifier is extracted from the video output information by the circuit shown in Figure 6. Transistors Q-8 and Q-9 are connected in a modified Darlington configuration to present a high input impedance to the video signal. The combination is biased on through R-28 as long as the voltage across R-26 is negative. As the anode of CR-3 approaches zero volts the diode is forward biased, turning Q-8 and Q-9 off, and allowing capacitor C-11 to charge through R-29, R-30 and CR-4. The discharge time constant of C-11 and R-31 is approximately 62 seconds so that C-11 will not discharge appreciably during the 2 second duration of a single scan. A second Darlington stage insures that the time constant is set only by the RC combination. Zener diode CR-5 prevents the capacitor from charging beyond its rated voltage in the event of a malfunction. The voltage swing across R-31 is further amplified and inverted by Q-11 and Q-12 such that a voltage swing of zero to -5 volts across C-11 appears as -20 to -5 at R-36. A 12 volt zener diode CR-7 performs a subtraction function so that the original zero to -5 volts signal now becomes -8 to zero volts. These values are actually adjusted so that a capacitor voltage of -1.5 to -4.5 volts results in a gate voltage of -6 to zero volts. Resistor R-18 and capacitor C-8 form a smoothing filter to prevent sudden fluctuations in voltage from reaching the AGC gate.

Thus it can be seen that, as the out-of-phase chopper signal is demodulated during "cold" scan periods, a positive d-c output will be present at the video output. This, then, causes C-11 to charge, applying a less negative voltage to the AGC gate. This positive-going voltage lowers the drain to source resistance of the field effect transistor, increasing the gain, and thus the signal injected into the log amplifier. Since it is a closed loop system, and cold space is viewed twice each scan period, a "reference level" is set at the chopper temperature.

### 2.3 Full-Time Telemetry

In order to meet the contract requirements for a full-time telemetering capability, a separate -20 volt regulator was added to the radiometer electronics. This regulator is fed directly from the full-time primary power bus, and its only functions are to supply power to telemetry circuits and also to power the cell temperature control circuit. The schematic diagram of this regulator is shown in Figure 7. The circuit is essentially the same as the -20 volt regulator used in previous flight models, with the addition of diode CR-1. This diode is a safety device which keeps the circuit from being damaged in case polarity of the input power is inadvertently reversed. The -20 volt (F/T) regulator is packaged in a module (Telemetry Module) along with Reference Temperature TM and motor TM circuits, located on the underside of the primary casting. In actual thermal vacuum tests, the -20 volt output varied from -21.15 volts at +50 degrees C satellite temperature to -20.72 volts at 0 degree C. This amounts to  $\pm 0.96$  percent about nominal +25 degrees C voltage.



14

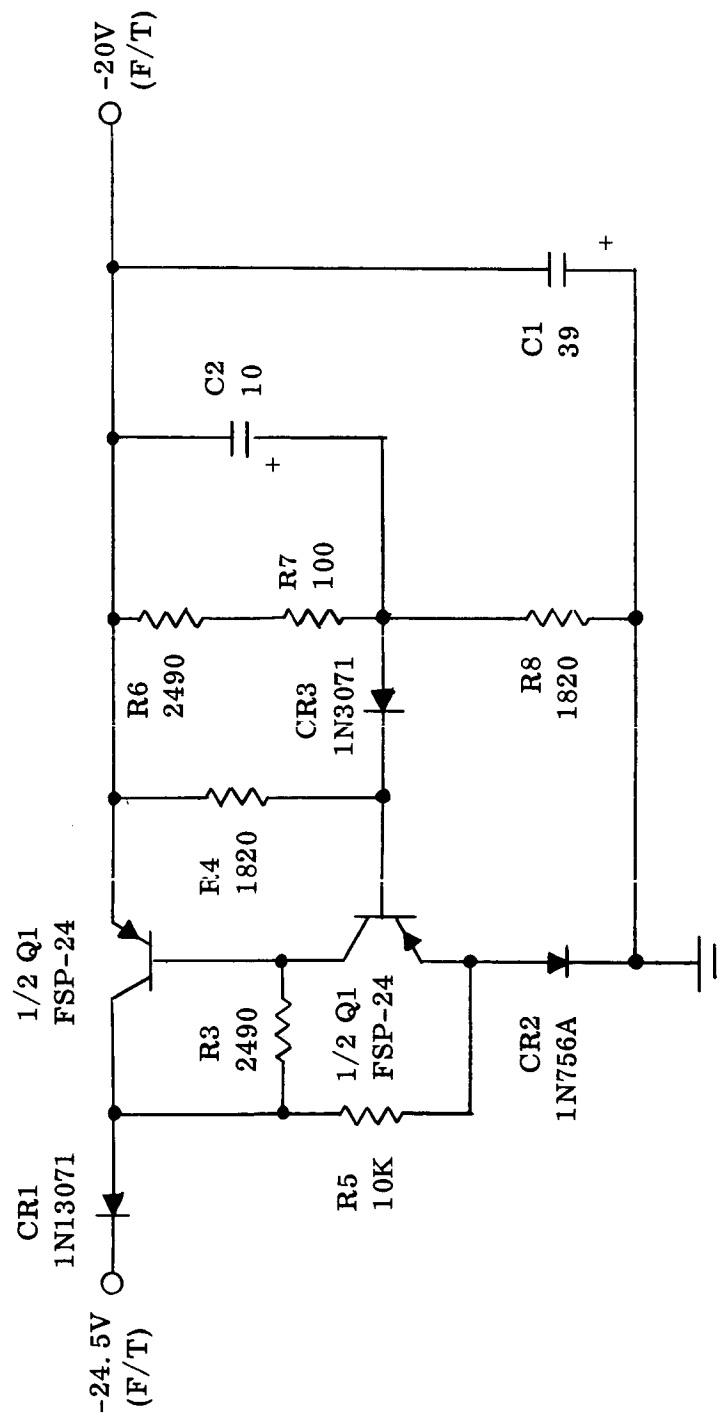


Figure 7 -20V F/T Regulator

Parameters selected to be telemetered are listed below:

1. Reference surface temperature "A"
2. Reference surface temperature "B"
3. Electronics housing temperature "E"
4. Detector cell temperature
5. Marker pulse
6. -20 volt regulator output
7. -20 volt (F/T) regulator output
8. Video signal output
9. Motor current
10. AGC gate bias voltage

Parameters and circuits of each point are detailed in the Telemetry Compendium, Appendix 6.2.

#### 2.4 Cell Temperature Control

As a result of the improvements in detector cooling (Section 3.0), the uncontrolled cell temperature assumes too low a value at the low end of the environmental temperature range (0 degree C to +50 degrees C). That is, the cell sensitivity passes through a maximum as a function of temperature, and the radiometer sensitivity varies as a function of the environmental temperature. For this reason, the Statement of Work calls for automatic control of the cell temperature such that cooling below -95 degrees C will not occur. The best control temperature is one at or near the maximum of cell sensitivity which can be maintained over the entire environmental temperature range. The temperature selected was -78 degrees C. With the improvements in the cooler, the temperature was maintained in the vicinity of -78 degrees C over the environmental range from 0 degrees C to +45 degrees C (Section 4.1). Before the cooling modifications were incorporated, the upper limit was about +15 degrees C.

The control circuit used on previous models (Figure 8) makes use of a 5.6 volt zener diode mounted on the cooling patch to provide heat and a control point. As the voltage drop across R-22, the thermistor, and Q-5 emitter base exceeds the zener point of the diode, it begins to draw current; this current then becoming proportional to the input voltage change. This type of current proportioning control is undesirable for two reasons:

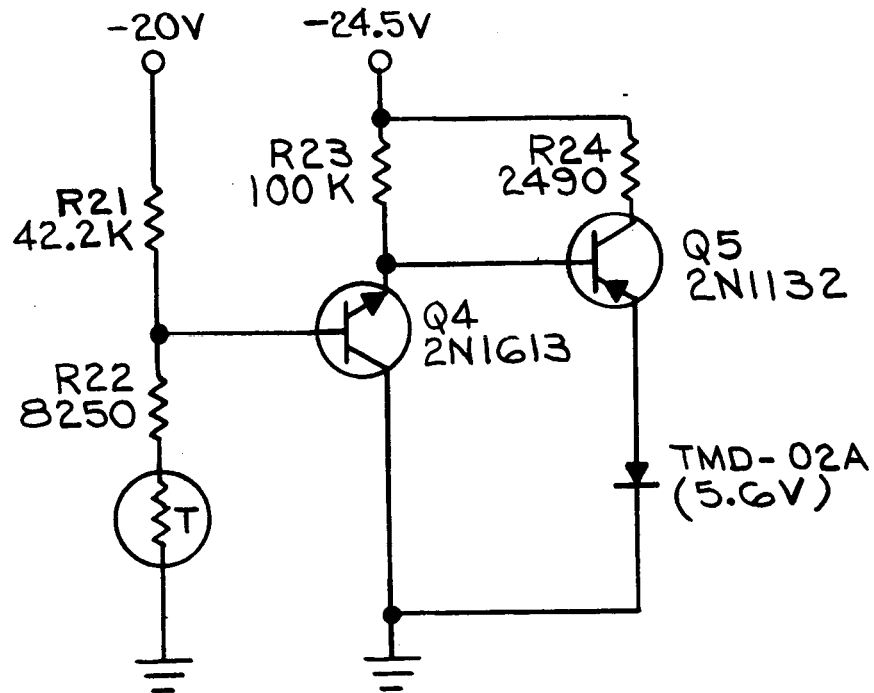


Figure 8 Original Cell Control Circuit

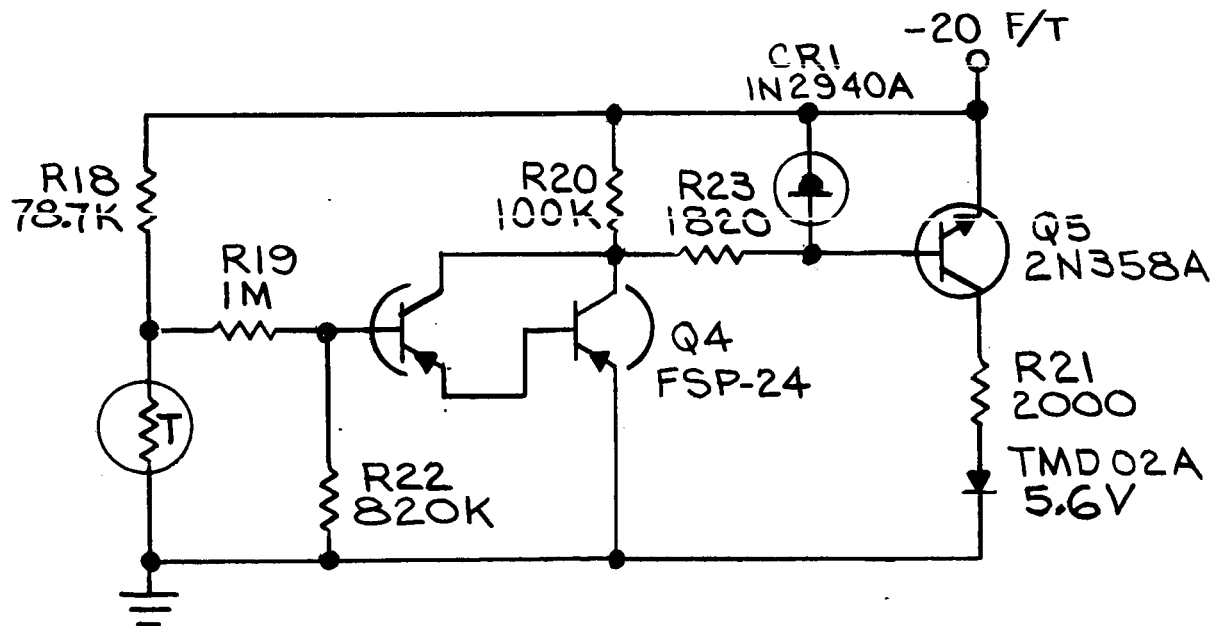


Figure 9 Improved Cell Control Circuit

1. Current (and thus power) is applied to the patch long before the equilibrium point is reached. This becomes a degenerative effect at higher ambient temperatures.
2. This type of circuit, because of relatively low gain, inherently requires rather large changes at the input to effect a small power increase at the diode. This has the effect of allowing rather large excursions in cell temperature at varying heat inputs to the cell.

In an effort to improve this situation, the circuit shown in Figure 9 was designed. This circuit uses an on-off current control principle, and makes use of the highly stable and fast switching characteristics of a tunnel diode to control the temperature set-point. Transistor Q-4 is a very high gain d-c amplifier in a modified Darlington connection. The gain of this stage is in the order of X1000, i. e., a change in cell TM voltage of 100 mv will cause a change of voltage at Q-2 collector of approximately 5 volts. Transistor Q-5 and tunnel diode CR-1 form a current sensitive switch. Q-5 remains in the "off" condition as long as the current through R-23 and Q-4 remains below the peak-point current of the tunnel diode. As this current increases beyond peak current, the tunnel diode switches to its high voltage state. At this point the major portion of current is diverted into the base of Q-5, causing it to switch to the "on" condition. R-21 serves as a current limiting resistor, holding the zener diode current to about 7 ma or 274 mw. The "on" to "off" hysteresis is about 100 mv, or 0.7 degree C. Action of this system is shown in Figure 10. The circuit operates from the -20 volt full-time regulator so that temperature control will not be lost during the daytime portion of the orbit.

## 2.5 Calibration Step Voltage

A calibration voltage at the radiometer output permits the easy and repeatable adjustment of the test and calibration recording equipment. A 0 to 6 volt calibration step voltage, in 1 volt steps, during one third of the housing (Reference Surface) scan is therefore called for in the specification. The following sections explain the generation of the step voltage beginning with its time positioning, and describe the results obtained during actual circuit operation.

### 2.5.1 Time Positioning

Since the only accurate measure of angular scan position is the synchronizing pulse train, this is the logical point at which to begin the timing of a calibration signal. The center of the "back" scan occurs approximately 1500 msec after the first synchronizing pulse, and its scan period extends about 150 msec either side of the center, or "straight up" position. Thus a delay of 1450 msec was introduced using a monostable multivibrator triggered from the Marker gate pulse. (See Figure 11). The trailing edge of this delay pulse triggers a monostable gate circuit which is used to turn on a 65 cps astable multivibrator for a period of 100 msec, or six pulses.



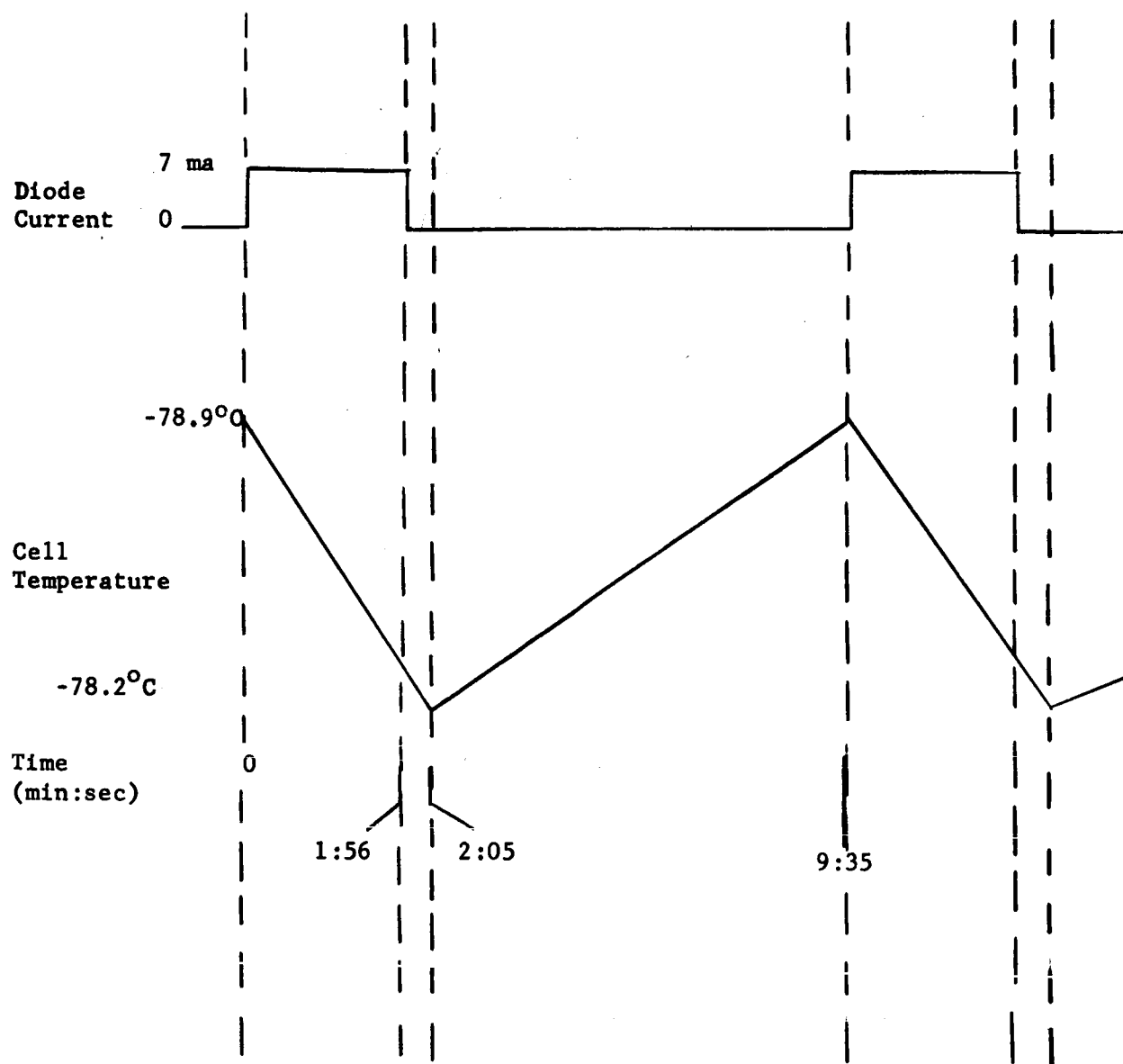


Figure 10 Typical Cell Temperature Cycling at 0°C

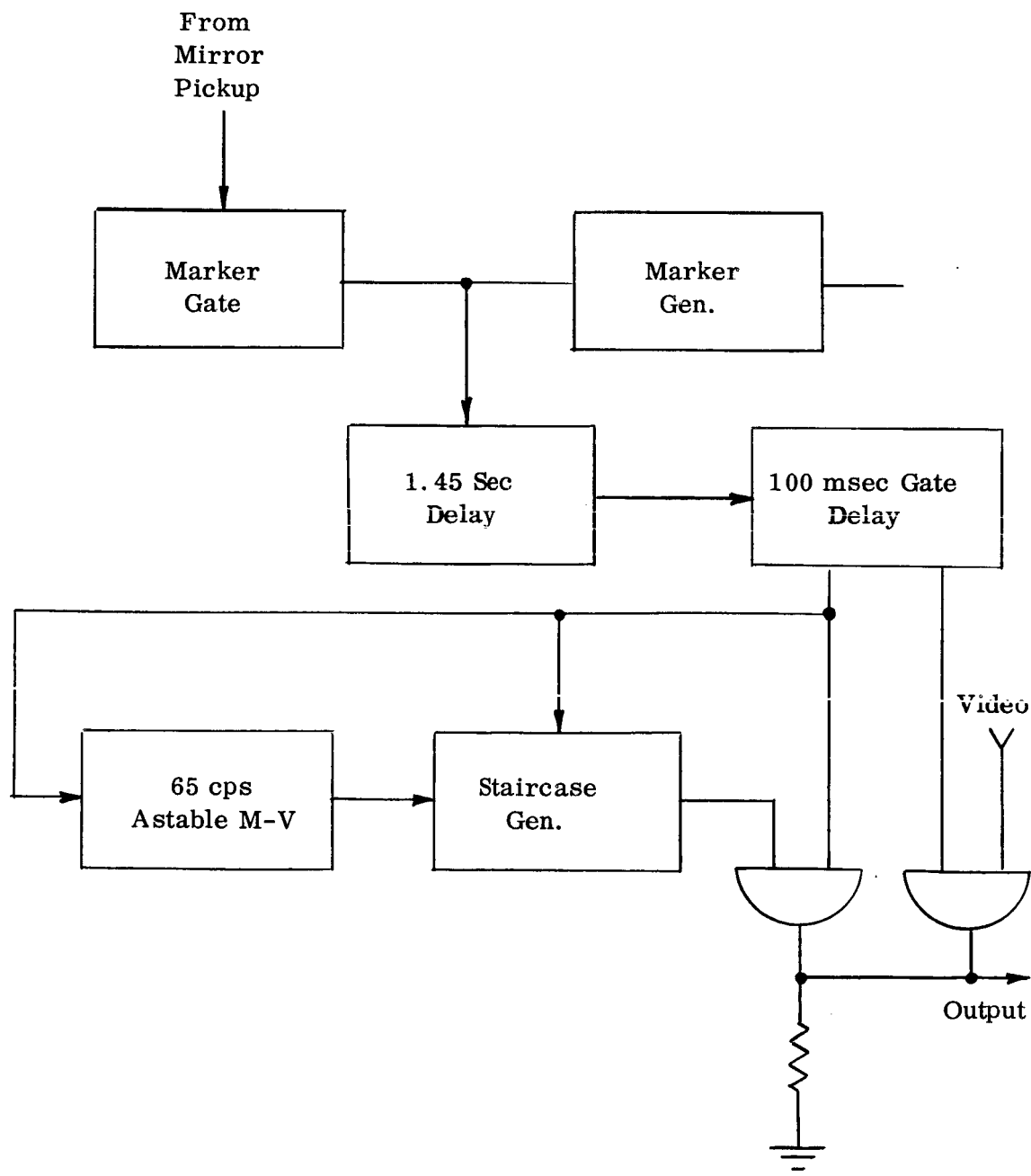


Figure 11 Block Diagram - Staircase Voltage Generator

### 2.5.2 Step Voltage Generation

These six pulses are then fed to the actual step-voltage generator, as shown in Figure 12. Operation of this circuit is dependent on the fundamental expression:

$$V = \frac{Q}{C}$$

where C = capacitance in farads

Q = charge in coulombs

V = potential difference in volts

Since charge is a measure of current and time, the expression may be written:

$$V = \frac{It}{C}$$

where I = current in amperes

t = time in seconds

Since, in the schematic diagram, Q-7 is essentially a constant current generator, and the value of C-10 is a constant, we have:

$$V \propto t$$

Now, if we can adjust the circuit values such that the period (t) of one pulse causes a voltage (V) of 1 volt, then each successive period (t) will cause an additional volt of potential to be added to the previous value, assuming negligible discharge between pulses.

Transistor Q-9 forms a very high input impedance d-c amplifier to minimize capacitor discharge and thus minimize "droop" between steps. Q-8 is used to fully discharge the capacitor between scans, and is triggered from the 1450 msec delay circuit. Resistor R-70 and sensistor R-29 are temperature compensating elements. The sensistor has a positive temperature coefficient and provides varying amounts of degenerative feedback to compensate for changes in transistor current gain with temperature.

Of particular concern was the temperature stability of the input capacitor C-9, which largely determines the magnitude of the input current pulses. In this regard a test was made of several types of capacitors at both temperature extremes. Results are shown in Table 1. As can be seen, the Scionics Type SCM demonstrated excellent stability throughout the range, and was chosen for use in this application.

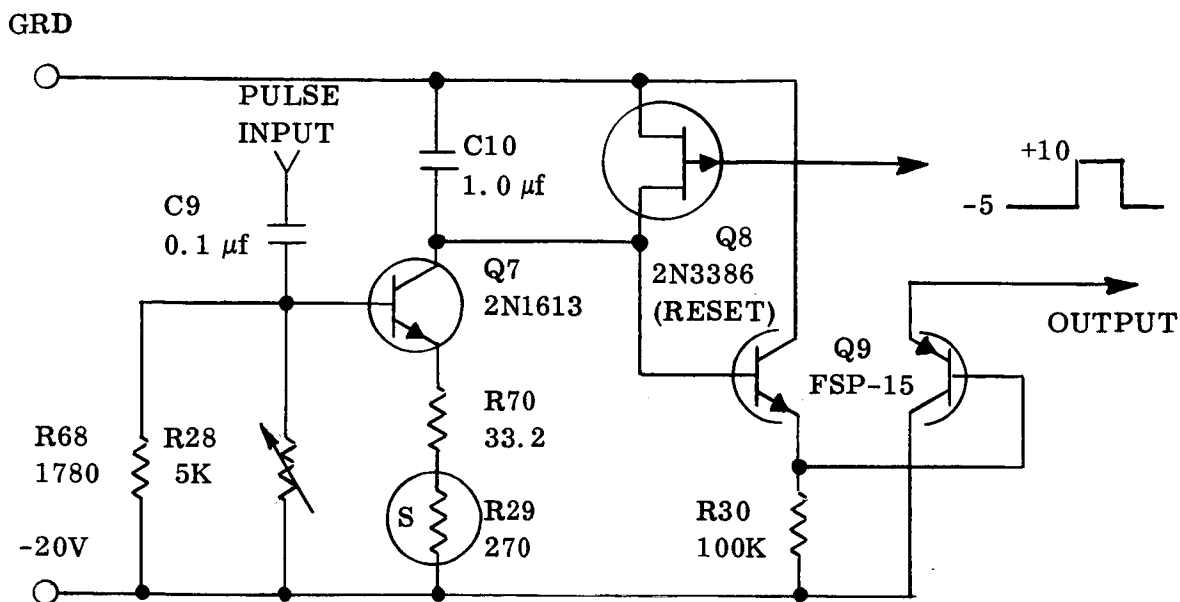


Figure 12 Staircase Generator Circuit

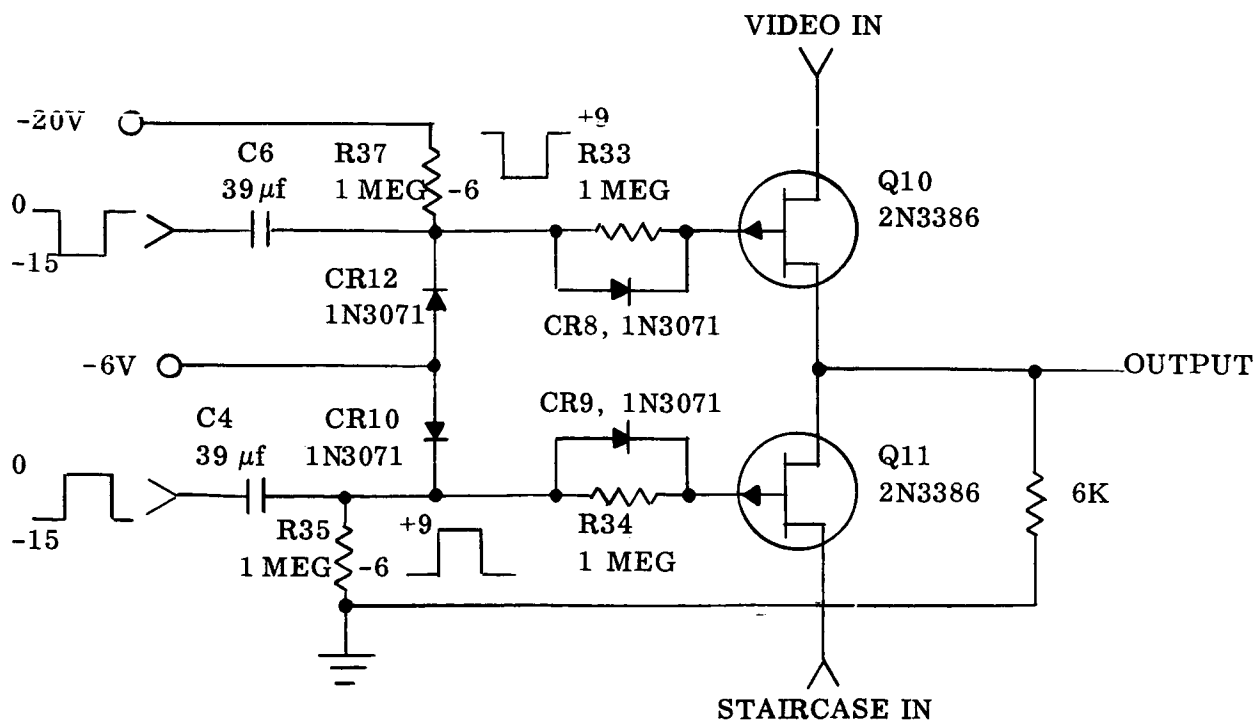


Figure 13 Transfer Gate Circuit

Table 1 Capacitor Temperature Stability Comparison

Temp. ( C)	Scionics SCM 30D	Hopkins P15P5D	Hopkins 1P2D	Sprague 114P1041R352	Good-All CP09A1KC104K	Cornell- Dubilier	Plastic Cap. AM2-104	T. I. SCM6
-30	.1000	.0915	.0895	.1020	.0940	.1000	.0975	.0833
-10	.1000	.0950	.0930	.1010	.0945	.1050	.0987	.0850
+10	.1020	.0970	.0950	.1020	.0945	.1022	.0995	.0880
+20	.1000	.0980	.0960	.1050	.0942	.1030	.1005	.0900
+40	.1000	.0985	.0975	.1000	.0945	.1030	.1005	.0930
+60	.0990	.1100	.0990	.1000	.0950	.1035	.1005	.0970

### 2.5.3 Multiplexing

In order to provide minimum loss and maximum isolation, a transfer gate system was required which would provide a low "on" resistance compared to the 6K load, and a very high "off" resistance to prevent crosstalk. A natural choice for this function was the field-effect transistor. The 2N3386 has a typical "on" resistance of 88 ohms, and an "off" resistance of approximately  $2 \times 10^9$  ohms. This causes only a 0.08 volt loss at 6 volts input.

The complete circuit of the transfer gates is shown in Figure 13. Pulses from the 100 msec gate multivibrator are sent through dc restorer networks to convert to bipolar signals required by the transistor gate electrodes. Since each transistor is fed from opposing sides of the gate multivibrator, the staircase voltage and the video signal are alternately placed on the 6K load resistor.

### 2.5.4 Results and Conclusions

Actual operation of the circuit has been, for the most part, quite satisfactory. A photograph of the actual step voltage signal, prior to multiplexing, is shown in Figure 14. A visicorder trace of the multiplexed video and calibration voltages is shown in Figure 15.

Temperature compensation is still somewhat lacking, due to nonlinearities in the transistor and sensistor characteristics. Additionally, a zero voltage point is not possible with this circuit. This, it is believed, is due to leakage current in the d-c amplifier, Q-9.

Since the original design was packaged, several new field-effect transistors have been developed. Among these is the CM603 which is an N-channel device having a typical "on" resistance of only 30 ohms. The N-channel configuration would also eliminate the need for a bipolar pulse input.

## 2.6 Scan Rate and Bandwidth Changes

The scan rate of 30 rpm was specified when an altitude of 750 nautical miles or 1373 kilometers was intended for Nimbus B. This altitude gives a sub-satellite velocity of 7.17 km/sec, and with the mirror rotation period of 2 seconds (for 30 rpm) it can be shown that the instantaneous angular field of view is 8.6 milliradians. The bandwidth for this field of view and mirror period is 184 cps.

### 2.6.1 Gear Changes

The scanning mirror speed was reduced to 30 rpm by changing the gear train to the configuration shown in Figure 16. The size of the mirror gear was increased, the ratios on the idler gear were changed, and the idler gear position was changed.

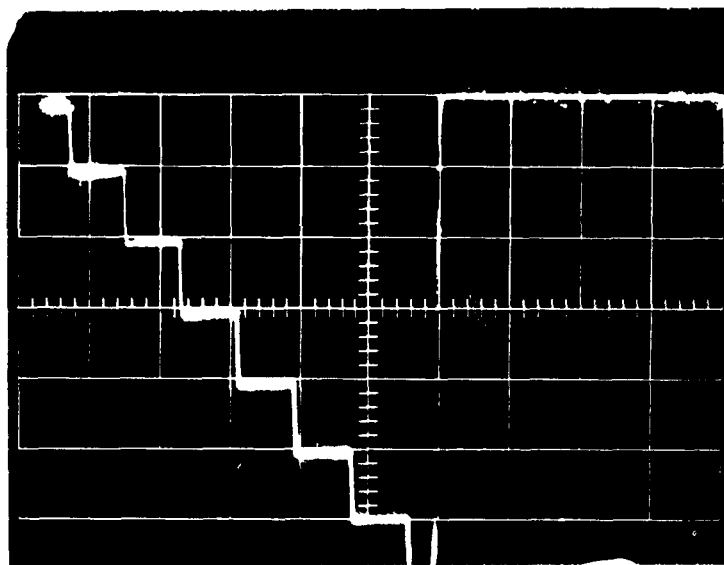


Figure 14

Oscilloscope Trace - Staircase Voltage

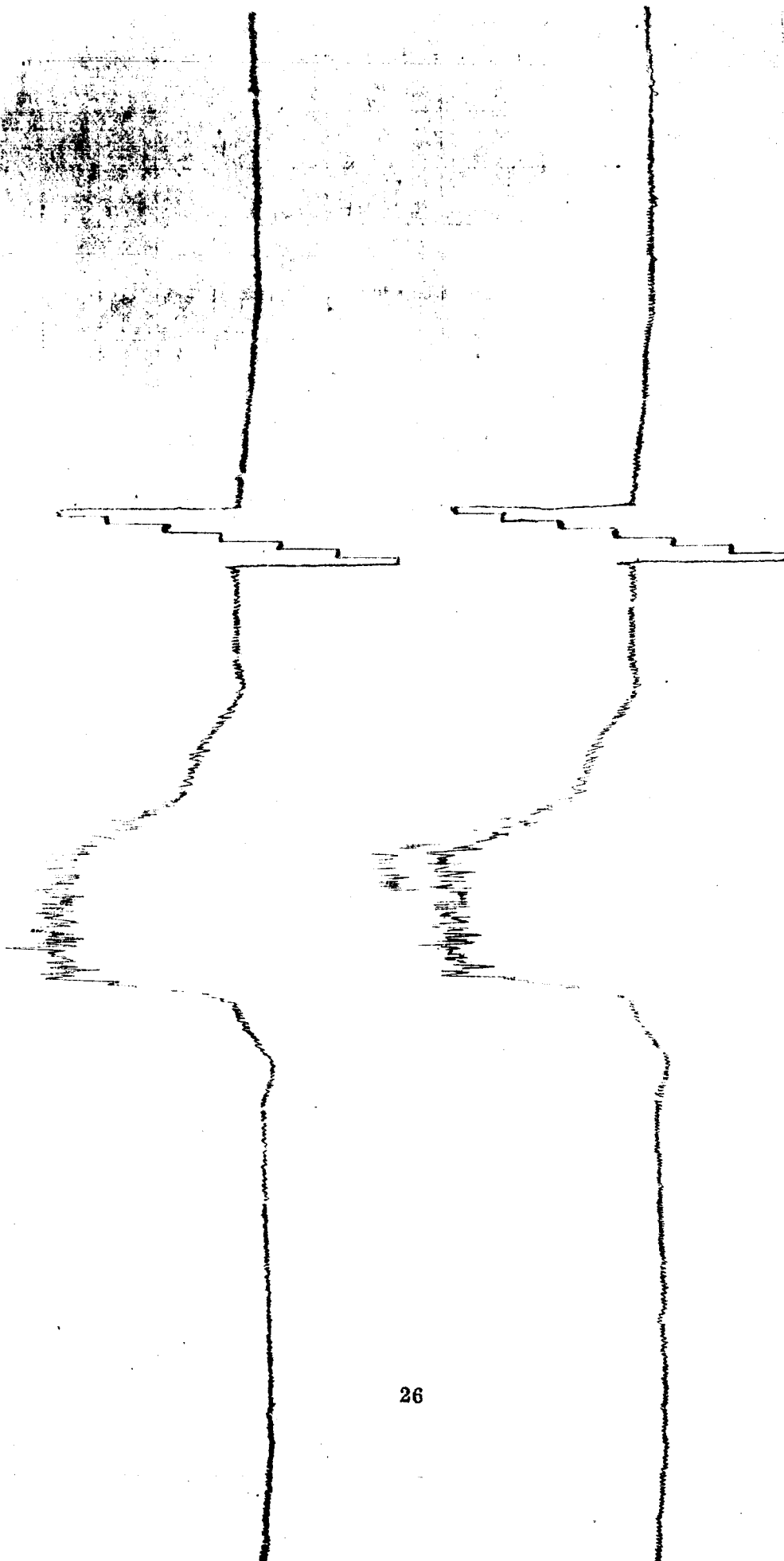
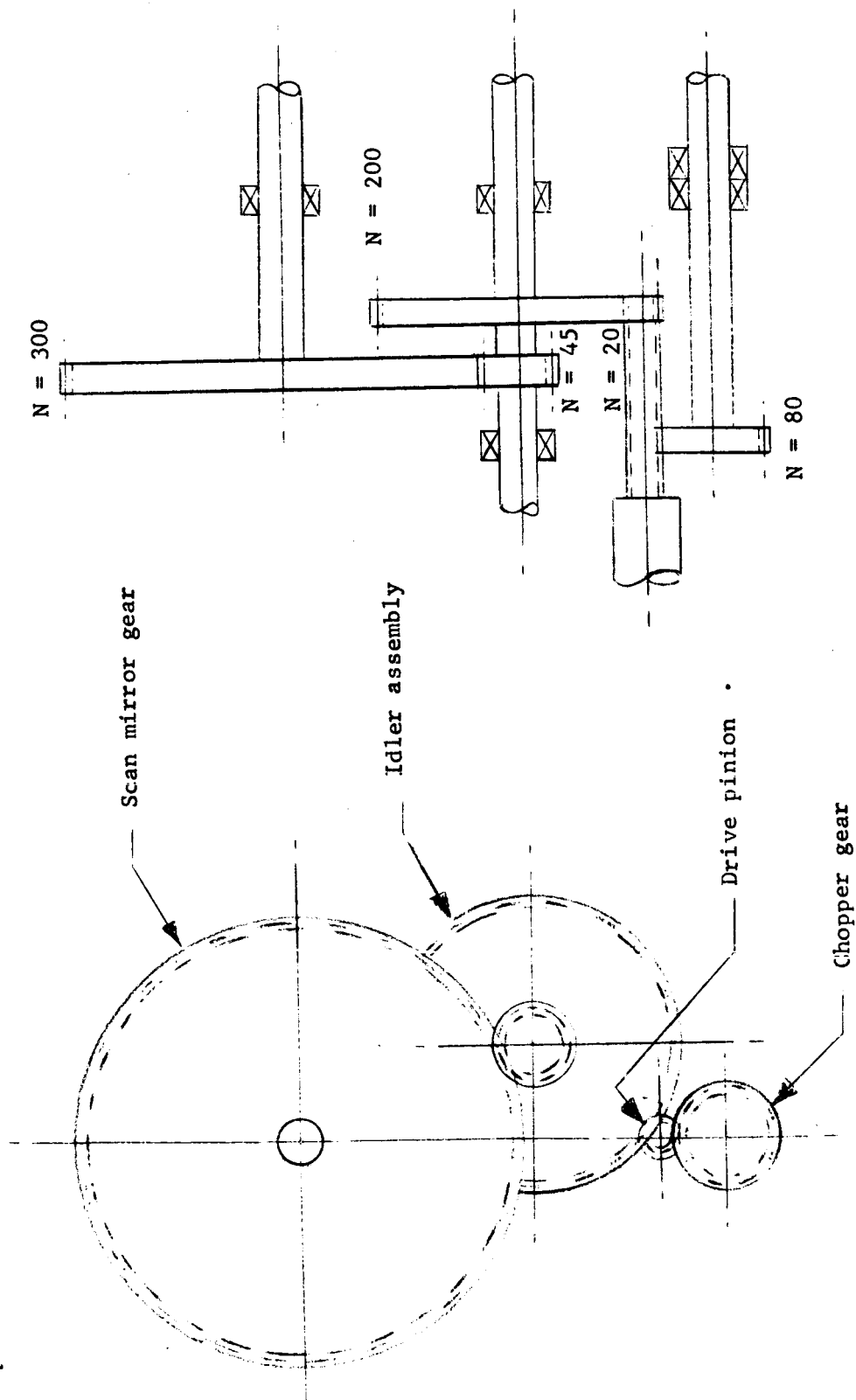


Figure 15  
Visicorder Trace Showing Staircase Voltage





NOTE: All gears 120 pitch

Figure 16 Scan Drive System for 30 RPM

To accommodate the changes of size and position, the motor mounting plate was redesigned and a new unit machined.

#### 2.6.2 Mirror Magnetic Pickup

The reduction in mirror rotational rate from 44.715 rpm to 30 rpm created a problem with the magnetic pickup used to trigger the marker pulse generator, since this device senses a steel slug on the scan drive gear. This reduction in speed was offset somewhat due to the increased diameter of the gear; however the calculations below show a 17.5 percent reduction in linear velocity of the gear slug. Since pickup output is directly proportional to speed, the resultant trigger pulse was reduced below a reliable value.

##### 1. Previous Models

Angular speed = 44.715 rpm (0.74525 rps)  
Slug rotational diameter = 1.75 inches  
Linear velocity =  $\pi(d) (\alpha \text{ speed}) = 4.1 \text{ inches/second}$

##### 2. Improved Model

Angular speed = 30 rpm (0.50 rps)  
Slug rotational diameter = 2.25 inches  
Linear velocity = 3.38 inches/second

A check with the pickup manufacturer (Electro-Products Corp.) revealed the availability of a new device, yielding nearly twice the output voltage under the same conditions. Package size of this pickup (No. 3025) is identical to the old unit. Use of this pickup has resulted in an over-all increase in the pulse amplitude of about 80 percent, providing even greater reliability than before. A secondary advantage was the allowable sensitivity reduction of the trigger circuitry, providing greater freedom from spurious noise triggering.

#### 2.6.3 Bandwidth Changes

The changes to a lower bandwidth, i. e., 184 cps instead of 277 cps, required a new low-pass filter. The filter received from our usual source was too large and cumbersome to be used. We therefore decided to design our own filter for use in this instrument. The resultant design is shown in Figure 17 while Figure 18 shows the response and delay characteristics. These characteristics were obtained using the demodulators so the results would be more authentic.

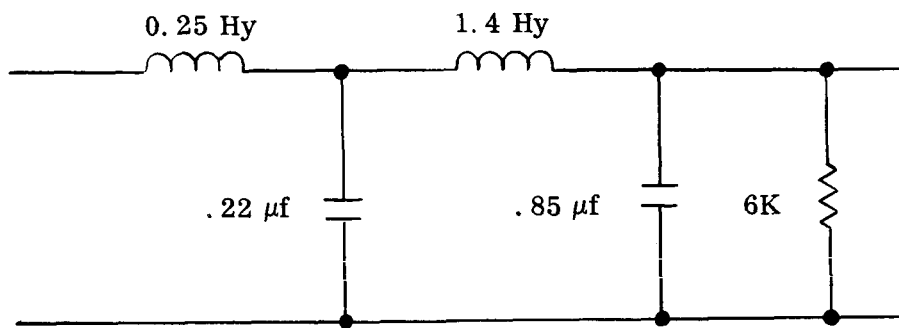
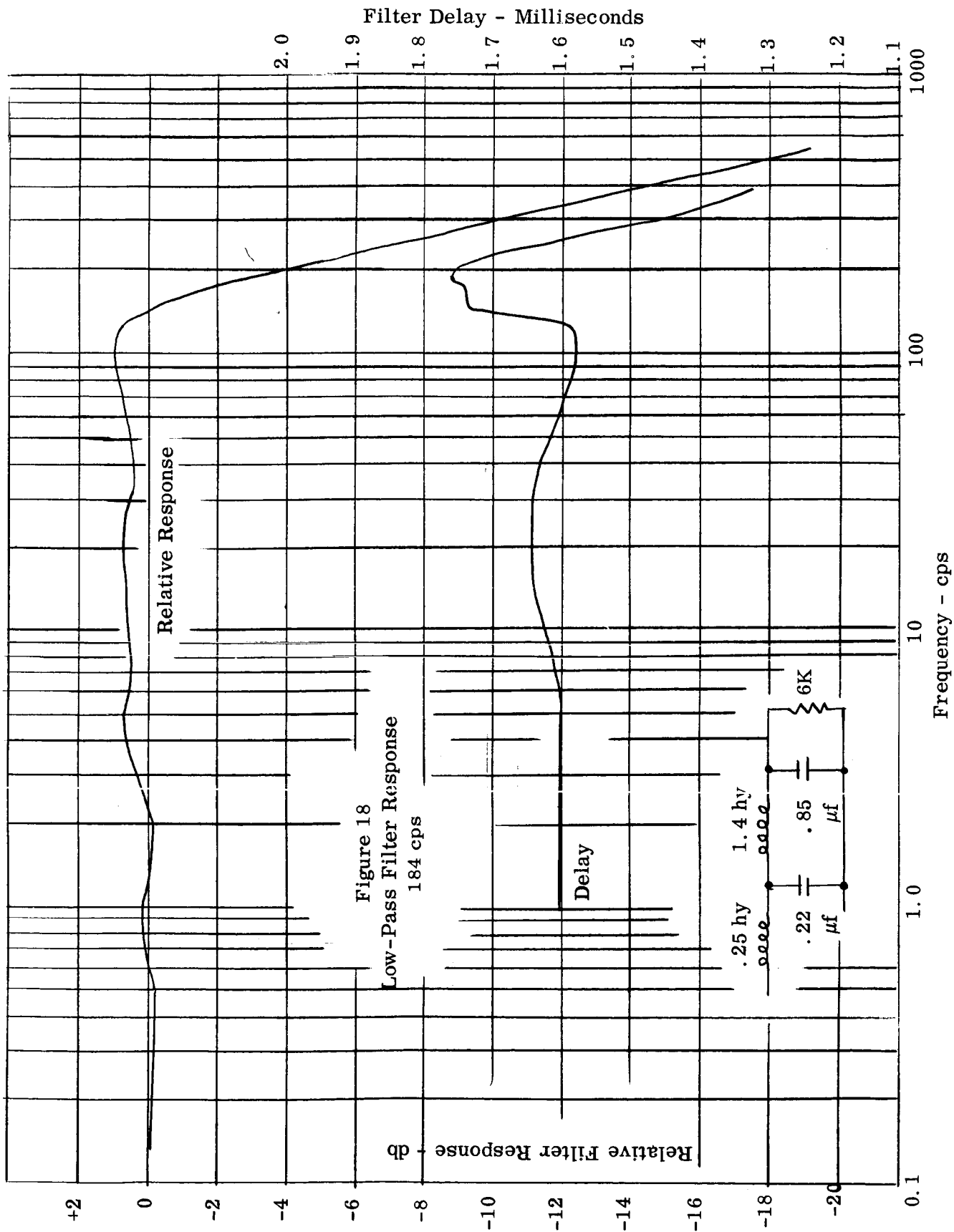


Figure 17 Low Pass Filter Circuit



### 3.0 DETECTOR COOLING MODIFICATIONS

In order to obtain the full advantage of a lower-noise preamplifier and electronic compensation of internally generated radiant signals, the detector must maintain its sensitivity over the temperature range of radiometer operation. This meant that the radiant cooler for the PbSe detector cell had to be improved. The purpose of the cooling modifications was therefore to develop a system with sufficient cooling capacity to insure proper cooling of the detector cell when the radiometer was subjected to the extremes of its anticipated operational temperatures. In approaching these modifications physical deviations with respect to size and innovations to existing hardware were circumvented and efforts concentrated in the areas of material changes and fabrication techniques.

The program was concentrated on those items in which obvious improvement could be made. These areas were the fiberglass casting, magnesium patch and cell holder, and the titanium support wires.

#### 3.1 Fiberglass Electronic Casting

In the normal operation of the HRIR it was known that the greater portion of all the energy supplied to the radiometer was dissipated into the magnesium castings. This additional energy, especially at the higher operating temperatures, resulted in a greater temperature gradient between the cell cylinder and the casting and thus a greater heat load through conduction and radiation coupling to the cell from the cell cylinder.

A very slight increase in cell cooling was observed during an experiment in which the electronic cans were isolated from the electronic casting. This increase was so insignificant that permanent isolation of the electronics would not be practical. From this experiment it was obvious that the thermal energy was being conducted from the main casting through the magnesium electronics casting. To verify this, another experiment was conducted in which the two castings were isolated by a low conducting material. This experiment showed a significant increase in cell cooling (-16.8 degrees C) even when the main casting was at 30 degrees C. A study based on these experimental results was made to determine the feasibility of constructing the whole electronics casting from a low conductive material.

This study was made and the material chosen was epoxy filled glass cloth, formed into the desired configurations by high pressure and stabilized by heat curing. Two well known companies who specialize in the manufacture of this type of material were consulted to assist in the exact choice of material and methods of fabrication. They were the Fiberite Corporation, Winona, Minnesota and the Synthane Corporation, Oaks, Pennsylvania. It was originally intended that the new electronics casting be molded in one piece. Due to the high cost of molds and extremely long delivery dates, an alternate approach was taken. This was to fabricate the casting in pieces

and then assemble as required. Of the above mentioned companies, only the Synthane Corporation had the facilities to fabricate from raw material stock.

Synthane proposed to fabricate and then assemble the casting as shown in Figure 19; which they did. Three of these castings were fabricated and delivered to ITTIL for evaluation. Prior to testing these castings, coil inserts were installed to provide a good threaded connection between the casting. Each casting was mounted to a main radiometer casting and vibrated at the prototype level. None of the new castings failed.

In comparing the fiberglass-epoxy material in the KIA magnesium alloy previously utilized, the following table may be used.

	<u>KIA</u>	<u>G-10</u>
Tensile Strength	24, 000 PSI	32, 500 PSI
Yield Strength	6, 000 PSI	19, 000 PSI
Specific Gravity	1. 80	1. 82
Thermal Conductivity (cals/sec·cm·°C)	0. 300	0. 0012

### 3.2 Titanium Alloy Support Wires

The wire suspension system which supports the patch and cell assembly provides a direct thermal link to the patch-cell cylinder. This thermal link reflects a higher cell temperature due to any increase in the temperature of the electronics casting. The suspension system consists of two separate three-wire assemblies shown in Figure 20. These assemblies are fabricated as shown in Figure 21.

Table 2 lists the properties of the several wire types considered, including Chromel AA. Since thermal conductivity was of prime importance, the titanium alloy was chosen for the modified Ti-130-1100-3AL suspension wires. This type of titanium alloy is not usually drawn into the 0. 009 and 0. 012 inch wire sizes required, so that obtaining a source of supply was a problem. The initial lot of wire tested was drawn by Fort Wayne Metals Inc. , Fort Wayne, Indiana, from 0. 030 inch stock received from Titanium Corporation of America. This lot was very brittle and could not be formed or worked. A second lot was ordered and was annealed in a vacuum furnace. Because of the residual drawing lubricants and their reaction with the wire at annealing temperatures, the wire lost most of its strength and was not usable.

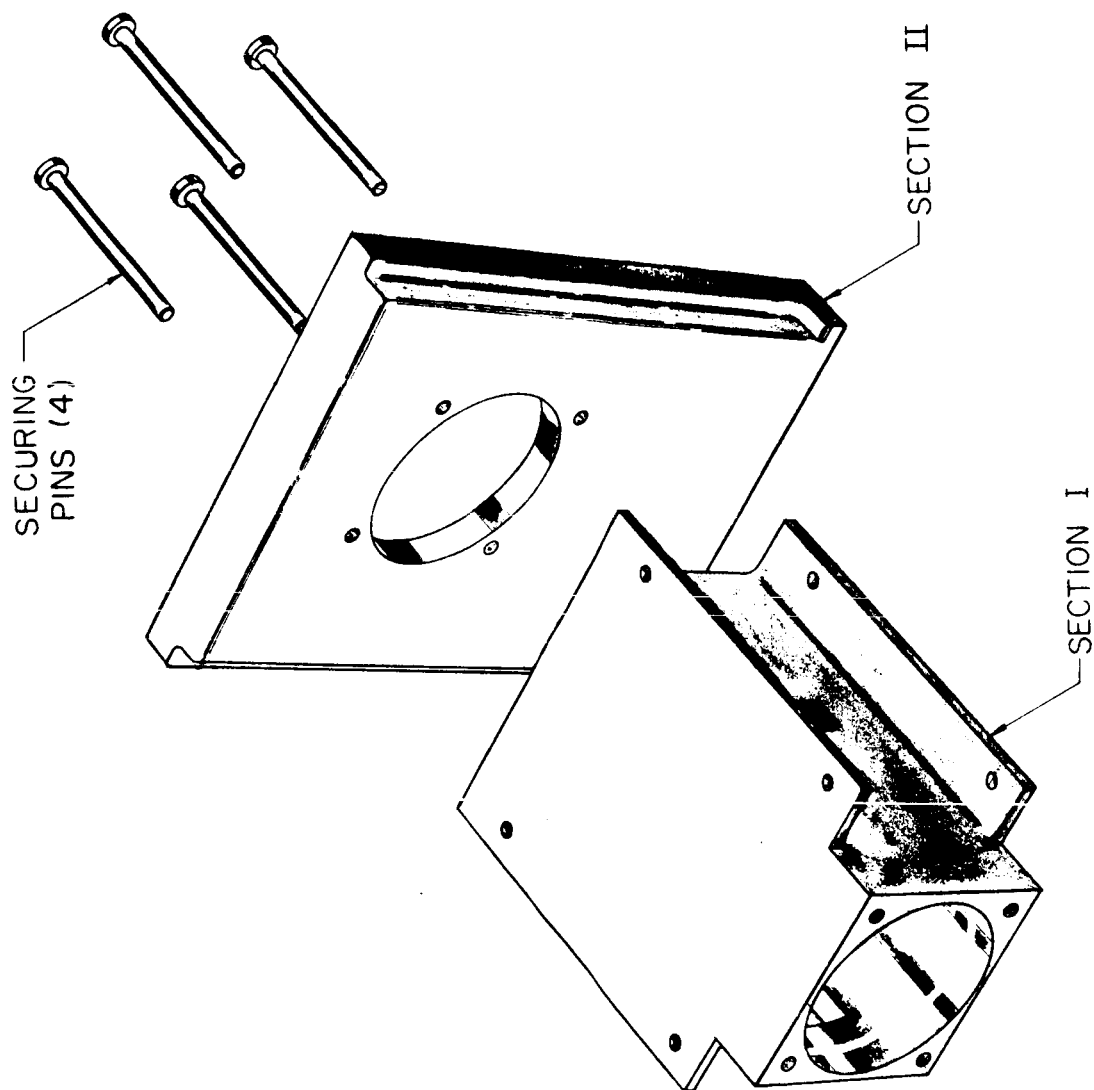


Figure 19 Synthane Casting Assembly

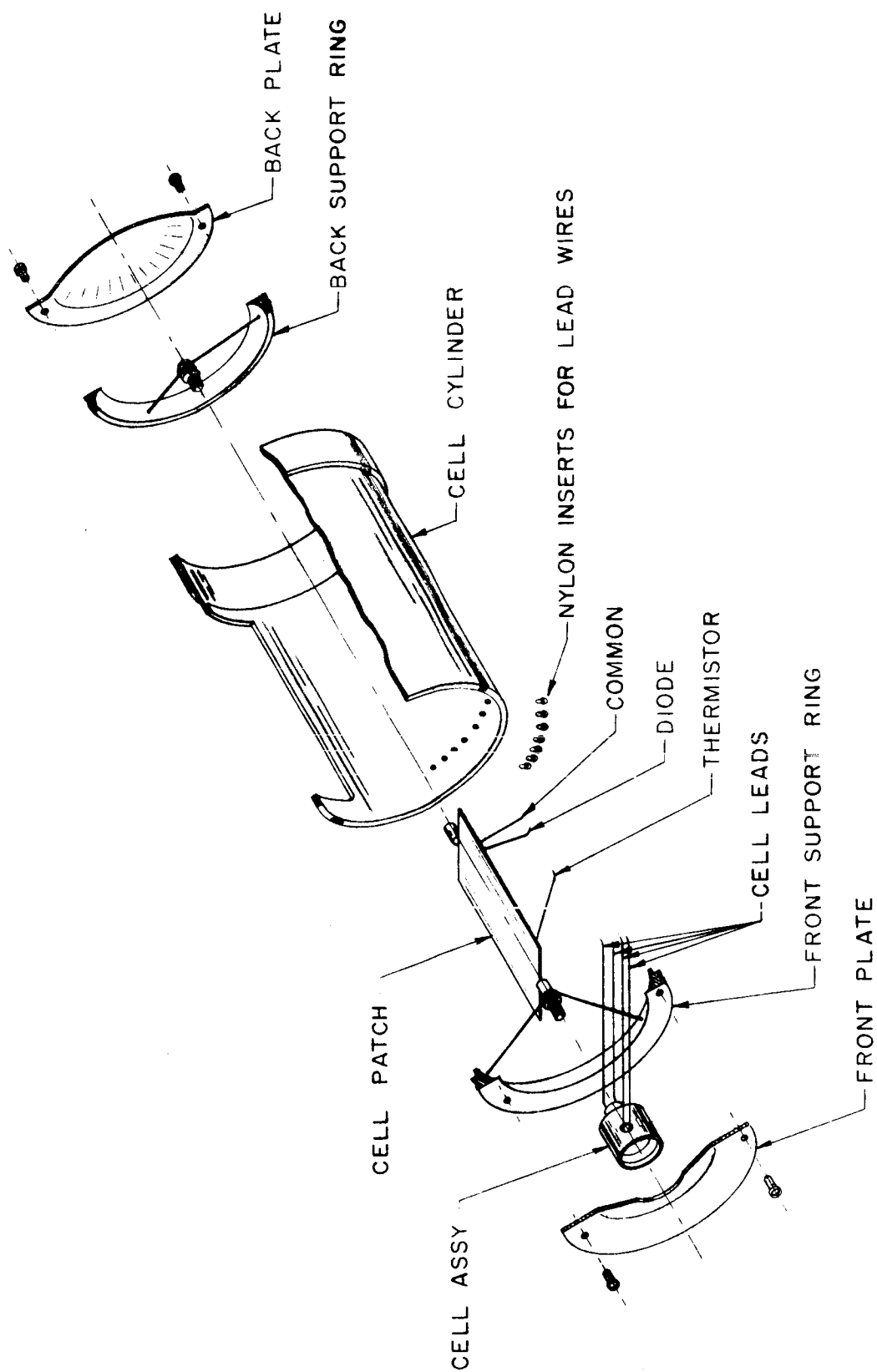


Figure 20 Radiation Cooler Assembly



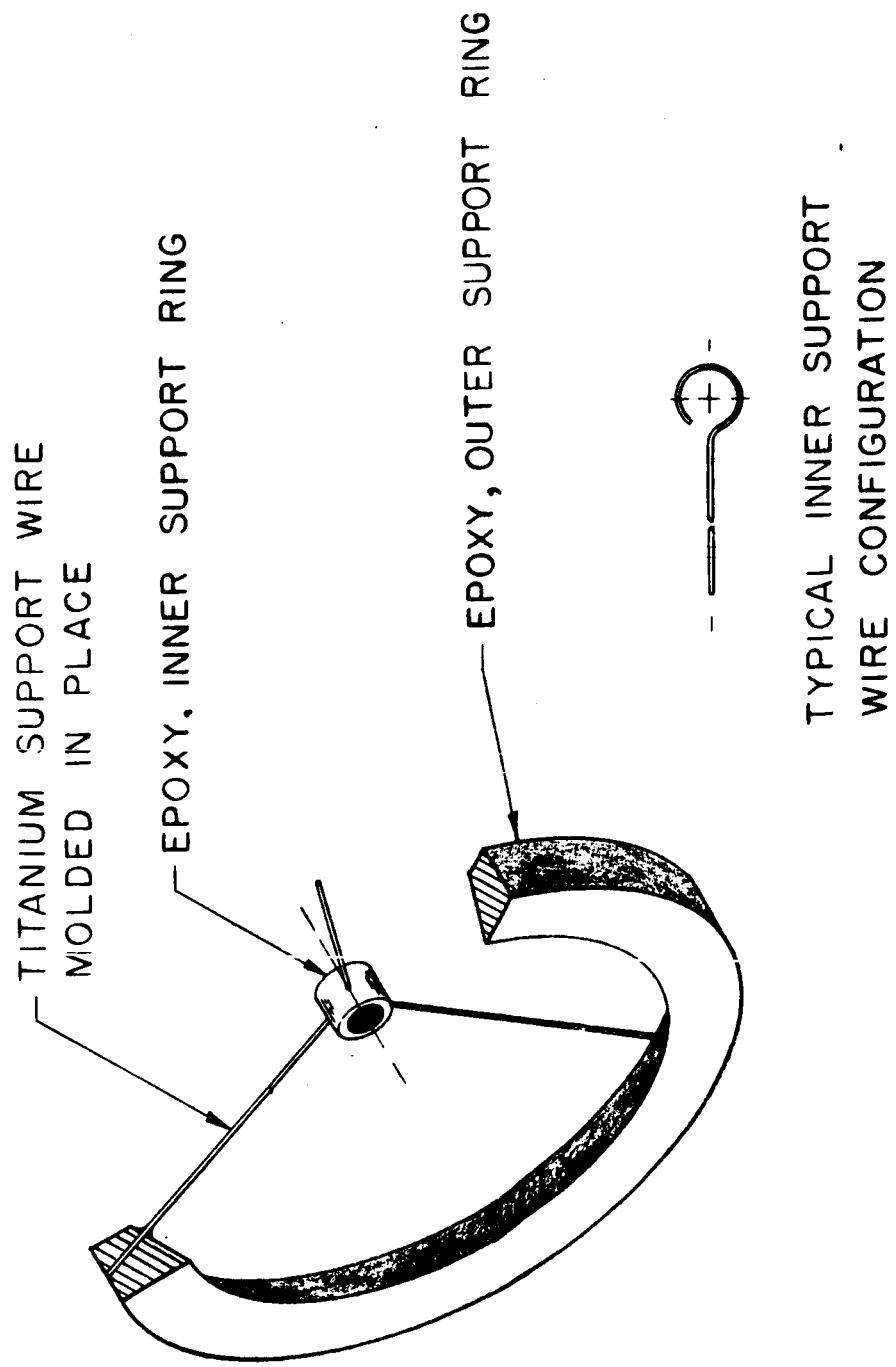


Figure 21 New Patch Suspension System

Table 2 Properties of Wire Types

	Chromel AA (Hoskins)	Nilvar (Driver-Harris)	Titanium 6Al-4V
Composition %	68 Ni, 20 CR, 8 FE	36 Ni, 64 FE	90 Ti 6Al 4V
Coeff. of Expansion	$13.5 \times 10^{-6}$ per °C (20° - 100° C)	$18 \times 10^{-6}$ per °C (700°C) $1.5 \times 10^{-6}$ per °C (0° - 100°C)	$10.4 \times 10^{-6}$ per °C
Specific Heat	0.107 cal/gram °C	0.123 cal/gram °C	0.135 cal/gram °C
Thermal Conductivity	0.13 watts/cm/°C (100°C)	0.105 watts/cm/°C	0.074 watts/cm/°C
Tensile Strength	130,000 psi	65,000 - 85,000 psi	145,000 - 180,000 psi (ht)
Yield Strength	90,000 psi (est. )	40,000 - 60,000 psi	135,000 - 175,000 psi
Elastic Limit	Not known	20,000 - 30,000 psi	-----

At this point, a suitable titanium alloy wire had not been found that could develop the desired mechanical strength. C. A. Roberts Company, who supplies titanium alloys, was therefore contacted to assist us in finding a company that could draw the type of wire needed. C. A. Roberts advised us to contact Astro Metallurgical Company in Ohio. Astro could and did draw two sizes of wire as requested, 0.009 and 0.012 inch diameters.

Titanium does not lend itself to easy fabrication by brazing or welding, thus it was decided that the wires would be looped, wrapped and secured by the use of epoxy. The most successful technique of looping and wrapping is shown in Figure 22. This method required extreme care in fabrication, and even then it did not insure an even distribution of stresses when assembled. Another method was tried, as illustrated in Figure 21. This suspension is assembled as shown with the aid of two sets of molds and jigs. Figure 21 shows the suspension system as it is presently constructed.

The testing configuration is shown in Figure 23 which also identifies the cell end and back end suspension rings. The vibration testing was conducted at 20 g between 5 to 2000 cps at a scan rate of 4 minutes per octave. Results are shown in Table 3.

From the test data, it is seen that the 0.009 inch diameter titanium wire was not at all suitable during the first few units. However, with improved techniques it may be seen that a 0.009 inch diameter wire could be used on the back end ring but not on the cell end. To enhance the mechanical characteristics, the 0.012 inch wire was used for both end rings. As shown in Table 3, there were no failures with this heavier wire. It should also be pointed out that during the fabrication period, the techniques of assembly were perfected to the point where no rejects were accounted for by the molding process.

### 3.3 Magnesium Patch

The use of magnesium was considered for the patch rather than aluminum to realize a significant weight saving. The comparative weights of the patch assemblies are as follows:

	<u>New</u>	<u>Old</u>
Weight of patch	1.71 grams (mag)	2.65 grams (al)
Weight of collar (threaded)	0.09 grams	.09 grams
Weight of collar	0.05 grams	.05 grams
Weight of control diode	<u>0.03 grams</u>	<u>.03 grams</u>
	1.88 grams	2.82 grams

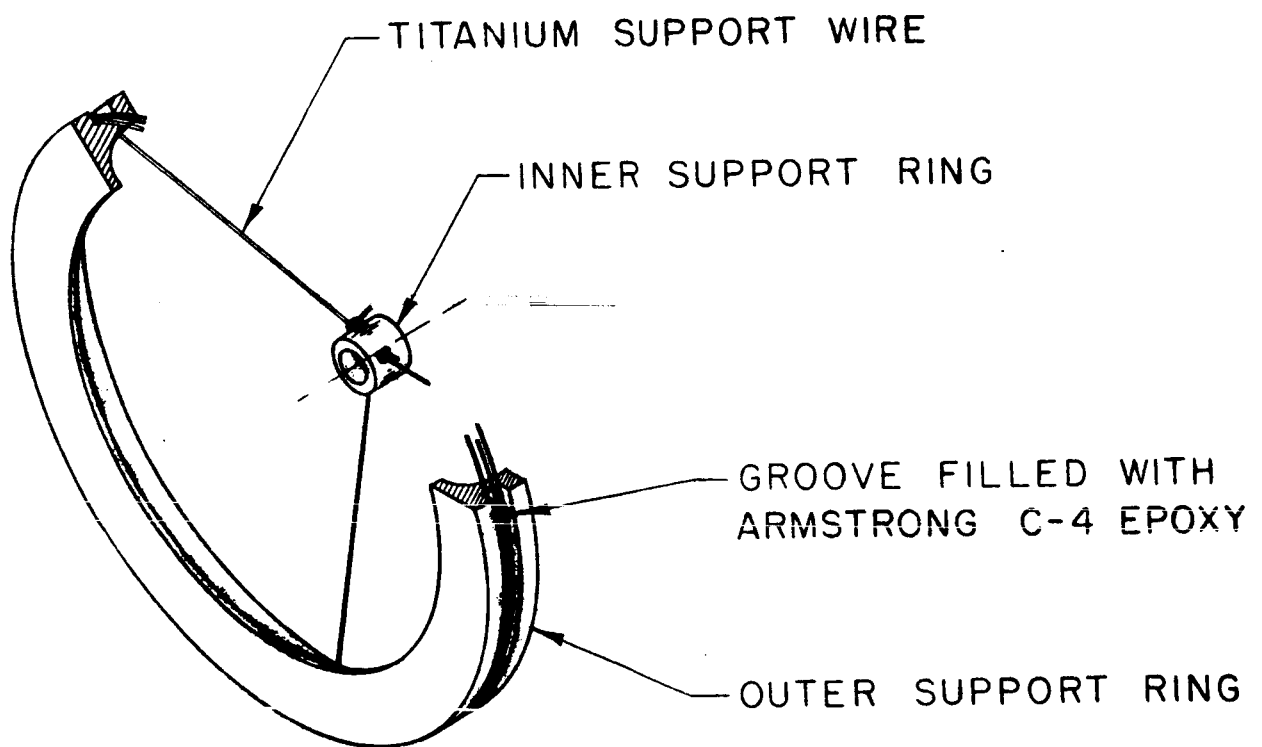
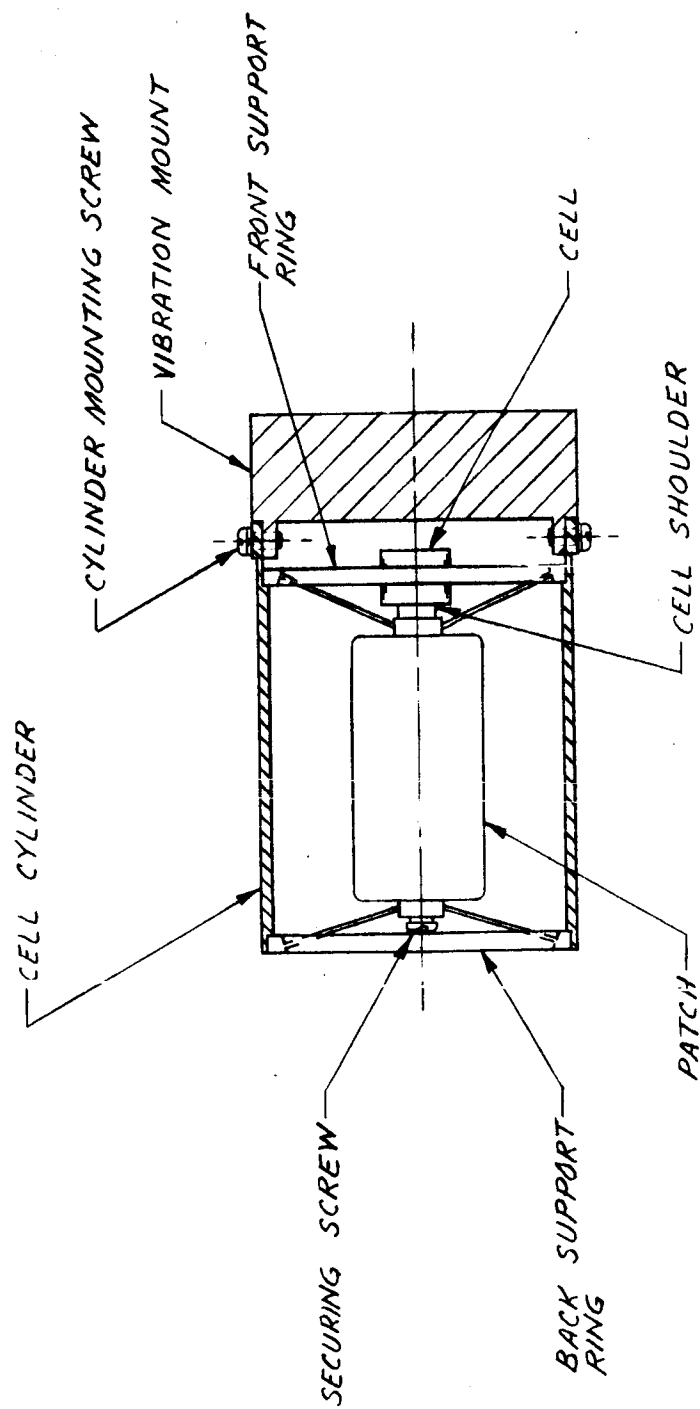


Figure 22 Alternate Patch Suspension Assembly



## VIBRATION TEST CONFIGURATION

Figure 23 Suspension System Test Configuration

Table 3 Vibration Test of Suspension Rings

<u>TEST NO.</u>	<u>DESCRIPTION</u>	<u>REMARKS</u>
1	Cell end ring made from 0.009 wire	Vibrated 1 hour. Resonance at 800 cps. No vibration damage. Wire pulled out of outer ring during assembly. It was noted that the wire ran through a small air bubble in the epoxy outer ring.
2	Back end ring made from 0.009 wire	Vibrated with No. 3, 4, 6, 7 with no apparent damage. Wire broke at 620 cps when vibrated with No. 9 on inner ring.
3	Cell end ring made from 0.009 wire	Vibrated with No. 2, wire broke on inner ring at 600 cps. Small nick in wire was noted.
4	Cell end ring made from 0.009 wire	Vibrated with No. 2, wire broke on outer ring at 650 cps. Epoxy chipped away at outer ring.
5	Cell end ring made from 0.009 wire	Failed during assembly.
6	Cell end ring made from 0.009 wire	Vibrated with No. 2, epoxy chipped at 500 cps on inner ring.
7	Cell end ring made from 0.009 wire	Vibrated with No. 2, epoxy chipped and released wire on inner ring at 520 cps.
8	Cell end ring made from 0.009 wire	Failed during assembly.
9	Cell end ring made from 0.009 wire	Vibrated to 620 cps when back end ring failed (No. 2). Vibrated again with an old ring (chromel AA) with no effects. Installed a new back end ring and No. 9 failed at 620 cps.
10	Back end ring made from 0.009 wire	Vibrated with No. 13, no damage. No. 13 was a cell end ring made from 0.012 inch wire.

Table 3 (Continued)

<u>TEST NO.</u>	<u>DESCRIPTION</u>	<u>REMARKS</u>
11	Cell end ring made from 0. 009 wire	Vibrated with No. 10 - failed at 570 cps.
12	Back end ring made from 0. 009 wire	No damage.
13	Cell end ring made from 0. 012 wire	Vibrated with No. 10 - experienced oil canning from 500 to 800 cps with peak at 620 cps. Recycled from 500 to 1000 cps noting some resonance points but no damage occurred. Revibrated with No. 14 resonance at 620 cps - no damage.
14	Back end wire made from 0. 012 wire	Vibrated with No. 13 resonance at 620 cps - no damage.
15	Cell end ring made from 0. 012 wire	Vibrated with No. 16 resonance at 620 cps - no damage.
16	Back end ring made from 0. 012 wire	Vibrated with No. 15 resonance at 620 cps - no damage.
17	Cell end ring made from 0. 012 wire	Vibrated with No. 18 resonance at 650 cps - no damage.
18	Back end ring made from 0. 012 wire	Vibrated with No. 17 resonance at 650 cps - no damage.
19	Cell end ring made from 0. 012 wire	Vibrated with No. 20 resonance at 590 cps - no damage.
20	Back end ring made from 0. 012 wire	Vibrated with No. 19 resonance at 590 cps - no damage.
21	Cell end ring made from 0. 012 wire	Vibrated with No. 22 resonance at 580 cps - no damage.
22	Back end ring made from 0. 012 wire	Vibrated with No. 21 resonance at 580 cps - no damage.

It is apparent that the reduction in the patch weight will reduce the g-force experienced during vibration and acceleration. This reduction will also increase the safety factor even if the old (chromel AA) suspension system is used. Magnesium has good dampening characteristics which should also assist in reducing the resonance g-force buildup. The final magnesium patch has the exact dimensional characteristics as the previously used aluminum model.

A completed assembly consisting of an epoxy casting, new titanium suspension system, and the magnesium patch was mounted to a main radiometer casting and vibrated at the prototype level 5 to 200 cps 4 minutes per octave. No signs of failure were noted. The system was considered mechanically sound.



#### 4.0 TESTS

A number of tests were performed to provide empirical justification of the theoretical improvements and to ensure conformance to environmental specifications. Since the Nimbus B environmental specifications were not available during the program, most tests were made to conform to "An Environmental Specification for the Nimbus Subsystems" dated April, 1961.

The results of performance tests and measurements on individual circuits are given in the sections describing the circuits. Specific test and measurement results are given in the following list.

<u>Circuit</u>	<u>Measurement</u>	<u>Figure and Section</u>
Low noise preamplifier	Noise figure versus source resistance	2, 2.1
Cell temperature control	Typical cell temperature control at 0 degrees C	9, 2.4
Calibration step voltage	Oscilloscope trace	13, 2.5
	Visicorder trace	14, 2.5
Low-pass filter	184 cps filter response	17, 2.6.3

The results of a series of vibration tests on various titanium alloy suspension rings are listed in Table 3, Section 3.2. The effect of all changes in the detector cooler are shown by the cooling test results given below (Section 4.1).

The field of view of measurements for the radiometer are given in Section 4.2. Sections 4.3 through 4.5 describe the humidity, vibration, and acceleration tests performed on the completed radiometer. The effect of all radiometer modifications, but especially the low-noise preamplifier, electronic offset, and cooler improvements, are reflected in the radiometric calibrations of the instrument given in Section 4.6.

##### 4.1 Cell Cooling Tests

A number of initial tests were run for the purpose of determining the effectiveness of the cell cooling improvements. Tables 4 and 5 summarize two representative tests of this nature. In all such tests thermocouples were placed at strategic points on the radiometer such that a temperature profile could be observed. No cell control was used in these early runs, and the cone shield was not in place.

Table 4 Cooling Run - August 17, 1964

Elapsed Time	Ref. A. Temp.	Cell Temp.	Satellite Temp.	Primary Cast. Temp.	Secondary Cast. Temp.
60	+34.1	-55.0	+51	+30.5	+13.5
75	+34.5	-59.6	+51	+30.8	+13.0
90	+34.6	-63.0	+52	+30.8	+12.0
105	+34.5	-65.9	+51	+30.0	+11.8
120	+34.6	-68.0	+51.5	+30.5	+11.5
180	+34.3	-72.5	+51.5	+30.0	+10.0
210	+34.1	-73.7	+52.0	+29.5	+ 9.5
240	+34.0	-74.6	+51.0	+29.5	+ 9.0
270	+34.0	-75.3	+52.0	+29.5	+ 8.5
300	+34.0	-75.9	+52.0	+29.5	+ 8.5
330	+34.0	-76.4	+51.0	+29.5	+ 8.0
360	+34.0	-76.8	+52.0	+29.5	+ 7.8
390	+34.0	-77.1	+52.0	+29.0	+ 7.5

Table 5 Cooling Run - August 19, 1964

Elapsed Time	Ref. A. Temp.	Cell Temp.	Satellite Temp.	Primary Cast. Temp.	Secondary Cast. Temp.
60	+13.7	-55.4	+17.5	+12.5	+9.0
75	+12.0	-61.7	+17.0	+10.8	+7.5
90	+10.8	-65.6	+17.0	+9.5	+6.2
105	+9.5	-68.9	+17.0	+8.5	+5.0
120	+8.7	-71.4	+16.5	+7.5	+4.0
135	+7.8	-73.1	+16.0	+7.0	+2.7
150	+7.2	-74.4	+16.0	+6.0	+2.2
180	+6.4	-76.4	+15.8	+5.2	+0.5
210	+5.5	-78.2	+15.5	+4.5	-0.5
300	+4.0	-82.1	+15.0	+3.0	-3.0
330	+3.5	-83.1	+15.0	+2.5	-3.7
360	+3.5	-84.0	+15.0	+2.0	-4.0
390	+3.2	-84.7	+15.0	+2.0	-4.7
420	+3.2	-85.3	+15.0	+2.0	-1.0

Later tests during calibration confirmed that cell cooling potential and speed were reduced somewhat by attaching the cone shield. Figure 24 shows cell cooling versus elapsed time for the early tests and also for two runs at 0 degrees C and +25 degrees C with the cone shield in place.

Table 6 compares the relative cooling capability of previous flight models to that of the Modified P-2 radiometer at three representative satellite temperatures. It can be seen that, using the synthane casting, Reference "E" temperature is relatively independent of satellite temperature, and that cell cooling is dependent primarily on Reference "E". Examination of these data will confirm that a vast improvement in cell cooling capability has been accomplished.

#### 4.2 Field of View Measurements

The focusing and field of view setting are accomplished simultaneously in our 100 foot long dark tunnel. The radiant source, a pinhole of light from a concentrated arc lamp collimated to a beam about 2 feet in diameter, is beamed into the optical cavity at the HRIR. The radiometer is then moved both vertically and horizontally in an angular fashion with respect to the beam. The output of the video amplifier is measured on an rms meter at intervals of the angular movement. A plot is made of output power versus the angular movement settings. This gives a plot of the instantaneous field of view. Since the detector converts radiant power directly into voltage, the 3 db radiant power points correspond to the 6 db electrical power points. Therefore, the width of the field of view is measured at the 6 db electrical power points on the curve. A plot of vertical and horizontal settings versus output follows in Table 7. Figure 25 is a curve of the relative response versus field of view. The vertical FOV is  $10.8 - 2.3 = 8.5$  mr and the horizontal FOV is  $10.3 - 1.75 = 8.55$  mr.

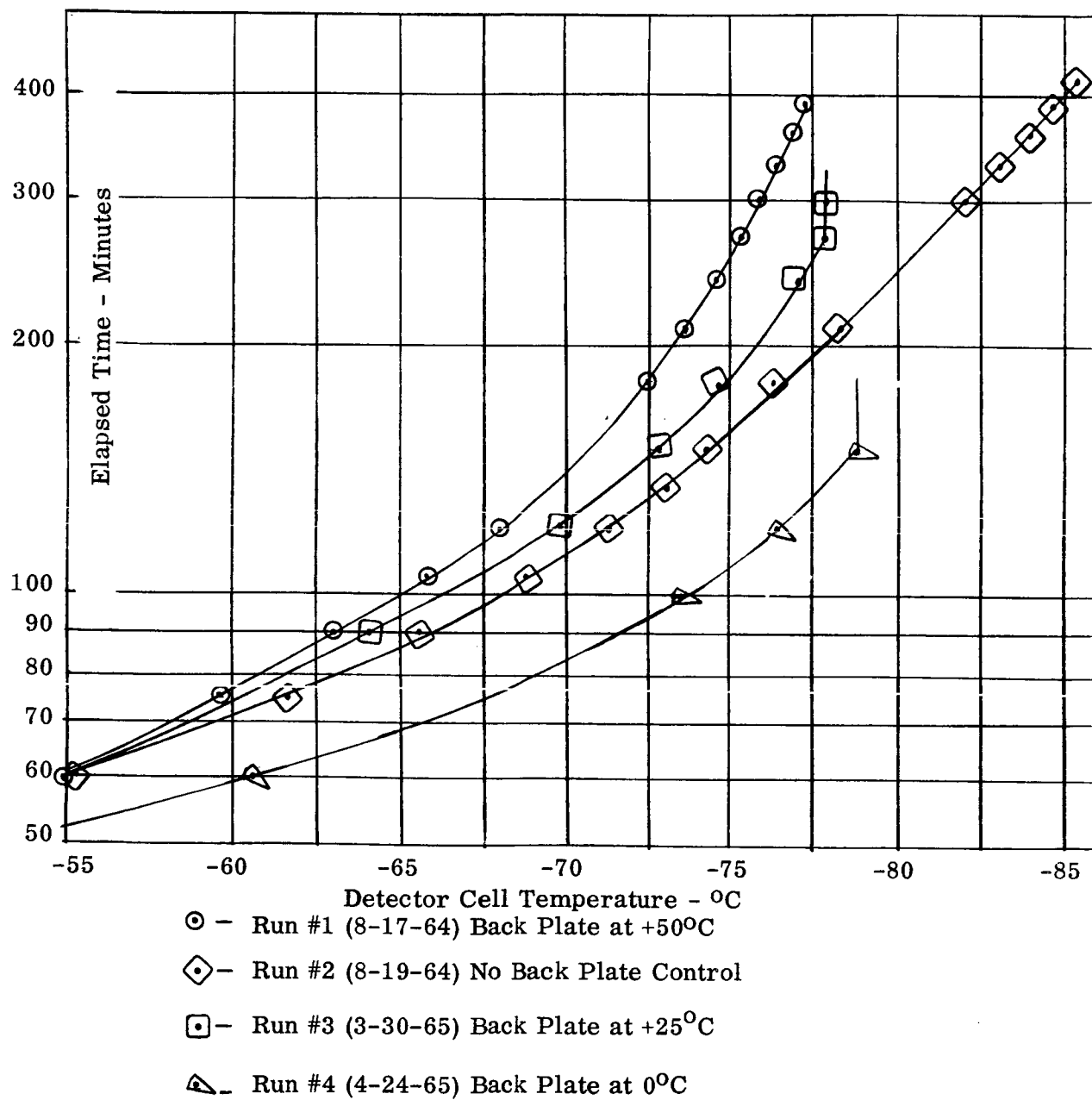


Figure 24 Cell Cooling Versus Time HRIR Radiometer Model P-2M/2

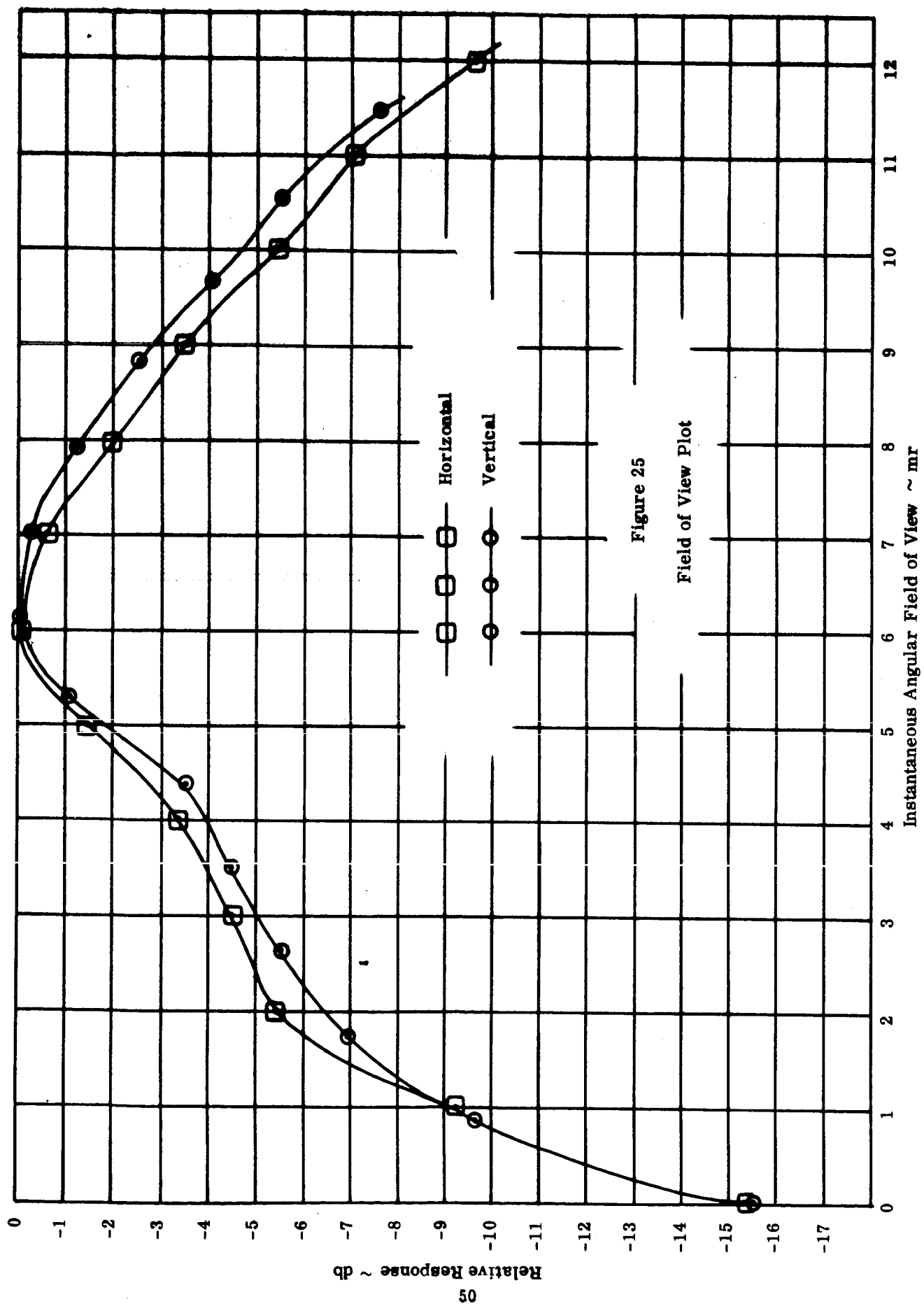
Table 6 Comparison of Cell Cooling Capabilities

Model	Satellite	Ref A	Ref E	Cell
F-1	+5°C	-0.6	+9.3	-73.1°C *
	+25°C	+17.5	+25.2	-64.6°C
	+45°C	+36.0	+39.8	-53.3°C
F-2	+5°C	0	+5.4	-75.8°C *
	+25°C	+14.2	+17.6	-70.2°C
	+45°C	+34.0	+34.0	-61.6°C
F-3	+5°C	+1.4	+8.5	-81.7°C *
	+25°C	+20.6	+22.1	-71.3°C
	+45°C	+40.0	+34.0	-60.1°C
F-4	+5°C	+3.0	+8.7	-76.2°C *
	+25°C	+21.3	+19.6	-74.1°C
	+45°C	+40.2	+33.0	-64.5°C
P-2	+5°C	+0.2	+16.0	-78.5°C *
	+25°C	+15.7	+16.2	-78.5°C *
	+45°C	+32.0	+21.5	-78.0°C *

\* Indicated controlled temperature

Table 7

Setting Milliradians	Vertical $E_O$ (Video Amp) db	$\Delta E_O$ db	Setting Milliradians	Horizontal $E_O$ (Video Amp) db	$\Delta E_O$ db
0	0	-15.5	0	0.8	-15.4
.88	5.9	- 9.6	1	7.0	- 9.2
1.76	8.6	- 6.9	2	10.8	- 5.4
2.64	10.0	- 5.5	3	11.7	- 4.5
3.52	11.0	- 4.5	4	12.9	- 3.3
4.40	12.0	- 3.5	5	14.7	- 1.5
5.28	14.5	- 1.0	6	16.2	0
6.16	15.5	0	7	15.6	- 0.6
7.04	15.2	- 0.3	8	14.2	- 2.0
7.92	14.3	- 1.2	9	12.7	- 3.5
8.80	13.0	- 2.5	10	10.8	- 5.4
9.68	11.4	- 4.1	11	9.2	- 7.0
10.56	10.0	- 5.5	12	6.0	- 9.6
11.44	7.9	- 7.6			





#### 4.3 Humidity

Prior to exposure to humidity conditions a cursory calibration was performed at +25 degrees C satellite temperature. This run is shown on pages 52 and 53. The radiometer was then exposed to 95 percent humidity at +40 degrees C for 50 hours continuous. After reducing the temperature to +25 degrees C, operation was checked and found to be normal. The test report is reproduced on page 54. The cursory calibration shown on pages 55 and 56 confirmed that no important change had taken place during humidity.

#### 4.4 Vibration

The post-humidity cursory calibration also served as the pre-vibration check. (See page 56.) The unit was then carried to GSFC for vibration testing which got underway on March 18. Due to uncertainty regarding new specifications for Nimbus B testing, it was decided to run this test at 15 g peak in the sine vibration mode at 2 octaves per minute (one 4.5 minute sweep). The test was begun in the thrust plane at 1151. After approximately 3 minutes of testing, it was noted that the mirror had stopped rotating while the chopper rotation was still normal. By turning the mirror manually it was evident that it was turning free without connection to the gear train. The cover was removed from the gear train, and a visual inspection revealed that the large gear of the idler gear assembly had slipped forward on its shaft, disengaging itself from the motor pinion.

The unit was returned to ITTIL where it was disassembled and the gear train inspected carefully. The failure was caused by slippage of the pressfit joint between the gear blank and shaft. A new gear assembly was modified by drilling and tapping the flange and gear to accommodate four 2-56 flat-head screws. The test and failure reports are reproduced on pages 58 through 62.

After insertion of this idler gear and reassembly of the gear train, a cursory calibration was performed to determine if any performance degradation resulted from vibration. There appeared to be a very slight phase shift in the chopper reference signal; however, as can be seen in the curve, this was not enough to affect performance. The cursory calibration is shown on pages 63 and 64.

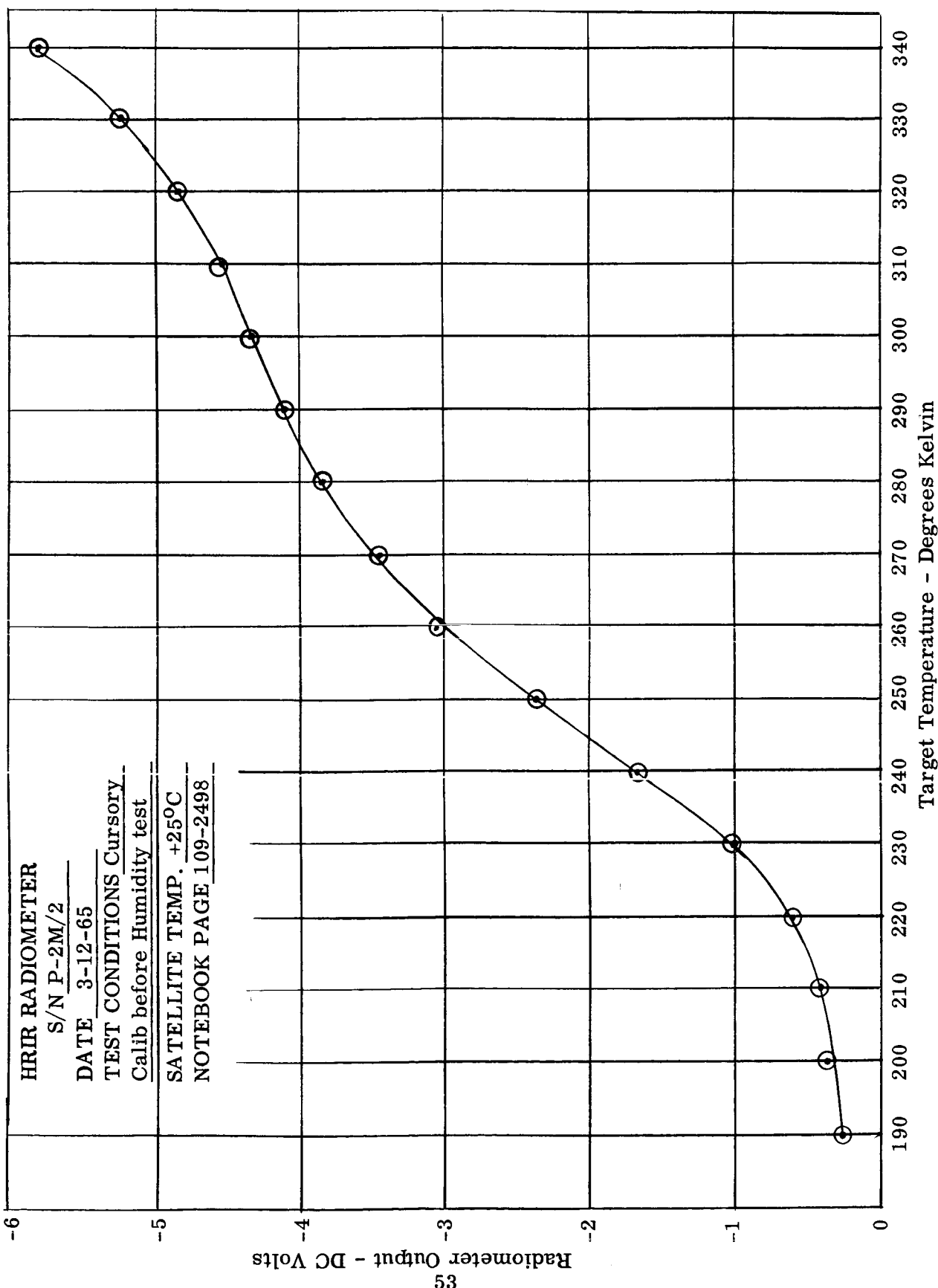
Another cursory calibration was run on March 30 in preparation for revibration at GSFC on April 2. (See pages 65 and 66.)

# Nimbus HRIR Radiometer Calibration

Date 3-12-65  
 Page 1 of 1

Type of Calibration: Initial Final 8 x 10<sup>-7</sup> Check before Humidity  
 Satellite Temperature +25 °C Pressure mm-hg  
 Data Booklet No. DB-P2M/2 HRIR Model and S/N Proto. - P2M/2 Cell Control  
 On - 2.19 V (78.6°C)  
 Off - 2.10 V (77.9°C)

Target (°K)	190	200	210	220	230	240	250	260	270	280	290	300	310	320	330	340
Target (°C)	-83	-73	-63	-53	-43	-33	-23	-13	-3	+7	+17	+27	+37	+47	+57	+67
Supply Voltage	24.6															24.6
Supply Current	130															130
-20 F/T TM	5.33															5.33
-20 Reg. TM	4.91															4.91
Ref A TM	3.84															3.68
Temp. (°C)	15.5															16.0
Ref B TM	3.94															3.77
Ref E TM	3.36															3.31
AGC TM	2.65															2.75
Cell TM	2.17															2.13
Temp. (-°C)	78.4															78.1
Marker Ampl.	5.75															5.65
No. Pulses	7															7
Marker TM	4.05															4.05
Motor TM	2.93															2.93
Target Signal	0.25	0.35	0.40	0.60	1.00	1.65	2.35	3.05	3.45	3.85	4.10	4.35	4.55	4.85	5.25	5.80



## TEST REPORT

### NIMBUS HRIR RADIOMETER - NASA

Contract No. NAS 5-3683


Model and Serial No: Pre-Prototype (P-2M/2)  
Test Environment: Humidity  
Date of Test: March 13-15, 1965 Test Run No. 1  
Tested by: ITT Federal Laboratories, Fort Wayne, Indiana  
Equipment Used: Tenney Climatic Chamber  
Method of Test: Maintain 40°C with 95% humidity for 50 hours continuous.  
Drop to 25°C with 95% humidity and check performance.  
Specification: "An Environmental Specification for Nimbus Subsystems"  
Reference Log Sheet Nos: Notebook 2498 - page 108  
Significant Results:

Unit operated normally after exposure with no apparent adverse effects.

Some white power deposits were noted on the casting, particularly the underside, however, these were not sufficiently serious to impair the operation or calibration of the radiometer. For the most part, these deposits can be removed by brushing with a stiff brush, leaving no serious permanent damage.

Conclusions: It may be concluded that radiometer operation will not be seriously affected by prolonged exposure to high humidity conditions. While it appears that the Dow 10 treatment is not 100 percent effective for humidity protection, it does reduce corrosion to the point where it no longer becomes a threat to operational reliability.

Recommendations: Based on results and conclusions as stated above, it is recommended that this report be accepted as a valid prototype qualification test under humidity conditions as stated in the environmental specification.

  
\_\_\_\_\_  
P. C. Murray  
Responsible Test Engineer

  
\_\_\_\_\_  
W. H. Wallschlaeger  
Project Manager

# Nimbus HRIR Radiometer Calibration

Date 3-16-65

Page 1 of 1

Type of Calibration: Initial \_\_\_\_\_ Final \_\_\_\_\_ Check \_\_\_\_\_ After Humidity \_\_\_\_\_ Step Voltage \_\_\_\_\_

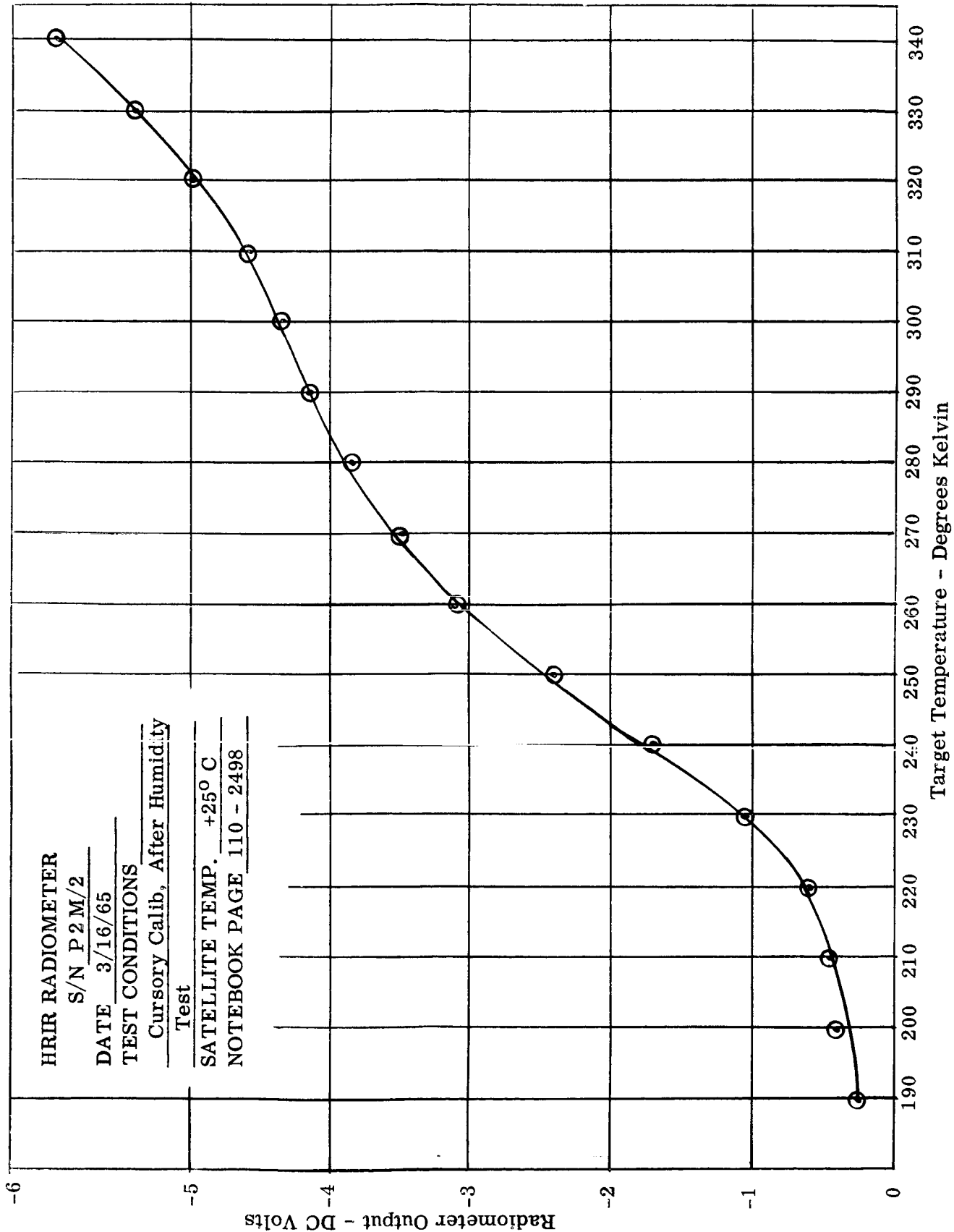
Satellite Temperature +25 °C Pressure 1 x 10<sup>-6</sup> mm-hg -5.95 V

Data Booklet No. DB-P2M/2 HRIR Model and S/N Prototype - P2M/2 Cell Control

On - 2.19 (-78.6°)

Off - 2.10 (-77.9°)

Target (°K)	190	200	210	220	230	240	250	260	270	280	290	300	310	320	330	340
Target (°C)	-83	-73	-63	-53	-43	-33	-23	-13	-3	+7	+17	+27	+37	+47	+57	+67
Supply Voltage	-24.6															24.6
Supply Current	133															133
-20 F/T TM	5.32															5.31
-20 Reg. TM	4.91															4.90
Ref A TM	4.01															3.85
Temp. (°C)	13.8															15.2
Ref B TM	4.12															3.96
Ref E TM	3.45															3.37
AGC TM	2.69															2.75
Cell TM	2.19															2.20
Temp. (-°C)	78.6															78.6
Marker Ampl.	-5.65															5.65
No. Pulses	7															7
Marker TM	4.05															4.05
Motor TM	3.15															3.10
Target Signal	0.25	0.40	0.45	0.60	1.05	1.70	2.40	3.10	3.50	3.85	4.15	4.35	4.60	5.00	5.40	5.95



After the cursory calibration on March 30, the unit was again carried to GSFC for vibration testing. On the morning of April 2, a low-level survey was run at 2g input to determine resonances and obtain a "Q" profile. In the afternoon, the radiometer was vibrated in sine and random lateral transverse axis, sine longitudinal transverse, and failed after 25 seconds of random vibration in the longitudinal axis. The mirror stopped turning and seemed to be blocked when it reached a point 90 degrees from nadir in the direction of the cooling cone opening. It appeared that the mirror magnetic pickup was hitting the gear slug at that point. The motor cover was removed, but the pickup appeared to be secure and well locked. The motor mount was then removed to reveal the gear train. An examination revealed that the scan mirror drive gear had slipped on its shaft away from the shaft flange. Testing was halted and the unit returned to ITTIL for repair.

On April 15, a meeting was held at ITTIL in Fort Wayne between NASA Technical representatives and ITTIL engineers to discuss the gear problem and evolve suitable solutions. It was generally agreed that the No. 6 press-fit used on all gear assemblies was inadequate, and that more secure methods of mounting the gears were necessary. Three methods were decided upon for the three assemblies, and these are illustrated in the failure report. In all cases, attachment between gear and shaft is made with screws. These "fixes" were implemented and the unit reassembled. The test and failure reports are reproduced on pages 67 through 74.

On April 23, a cursory calibration was made at a satellite temperature of +25 degrees C. This curve indicates no important deviation from previous calibrations. (See pages 75 and 76.)

On April 30, the radiometer was once again carried to GSFC for vibration testing. The unit was vibrated in sine and random, thrust and longitudinal axes, with the only incident occurring when the scan mirror set screw was noted to be loose after both sine and random longitudinal tests. During the lateral sine test the mirror stopped at 145 cps and the test was halted. The castings were separated and it was noted that the relay mirror aperture had come loose, causing the chopper to jam. The aperture was removed and the unit reassembled. Since loc-tite was not immediately available, it was decided to resume testing without loc-tite on the casting screws. The lateral sine and random tests were then run without further incident. It should be noted here that the relay apertures which failed has been proved superfluous, and as such will be left out of the unit. Upon return to ITTIL all screws which were removed were treated with "yellow" loc-tite, including the scan mirror set-screw. The test report is reproduced on pages 78 and 79.

## TEST REPORT

### NIMBUS HRIR RADIOMETER - NASA

Contract No. NAS 5-3683

Model and Serial No: Pre-Prototype (P-2M/2)  
Test Environment: Sinusoidal Vibration  
Date of Test: March 18, 1965 Test Run No. 1  
Tested by: NASA-GSFC (T & E Branch)  
Equipment Used: MB C-50 Electronic Shaker System

Method of Test: Cycle from 24 cps - 2000 cps at 0.25 single amplitude, three planes. 15 g (0-pk). One 4.5 minute sweep at 2 octaves/minute/plane.

Specification: "An Environmental Specification for Nimbus Subsystem"

Reference Log Sheet Nos: SVE-2m and failure report attached.

#### Significant Results:

Testing was initiated at 1151 in the thrust plane and terminated at 1155 due to failure within the scan mirror drive system.

Disassembly of the gear assembly indicated that the idler gear had separated longitudinally on its shaft causing it to disengage from the motor pinion. Repairs were performed (see attached failure report) and a cursory calibration test made. This check indicated no detrimental effect of vibration on the instrument calibration.

P. C. Murray  
P. C. Murray  
Responsible Test Engineer

W. H. Wallschlaeger  
W. H. Wallschlaeger  
Project Manager



## FAILURE REPORT

Date March 18, 1965 Time of failure 1155  
Project No. 11-20752 Other Reference HRIR (Modified)  
Contracting Agency NASA-GSFC Contract No. NAS 5-3683  
ITTIL Dept. No. 6130 Project Manager W. Wallschlaeger

Type of Failure: (Check Two)	Component <u>X</u>	Mechanical <u>X</u>
	Subsystem <u>          </u>	Electrical <u>          </u>
	System <u>          </u>	Optical <u>          </u>
	Other <u>          </u>	Other <u>          </u>

Specify: Model or Part No. 4708138 Serial No. None

### Test Conditions at Time of Failure:

The unit was undergoing sinusoidal vibration in the thrust plane at 15 g peak amplitude. Frequency cannot be pin-pointed, but was in the vicinity of 1000-1500 cps.

### Nature of Failure:

During vibration, the scan mirror stopped rotating, however the chopper remained operating. By manually turning the mirror it could be seen that it was not connected to the gear train.

### Cause of Failure (if known):

The failure was caused by longitudinal separation of the large aluminum gear from its shaft flange. This separation caused it to become disengaged from the motor pinion, allowing the mirror to "run free". See Figure 1 for a comparison of the defective gear (left) and a good gear (right).

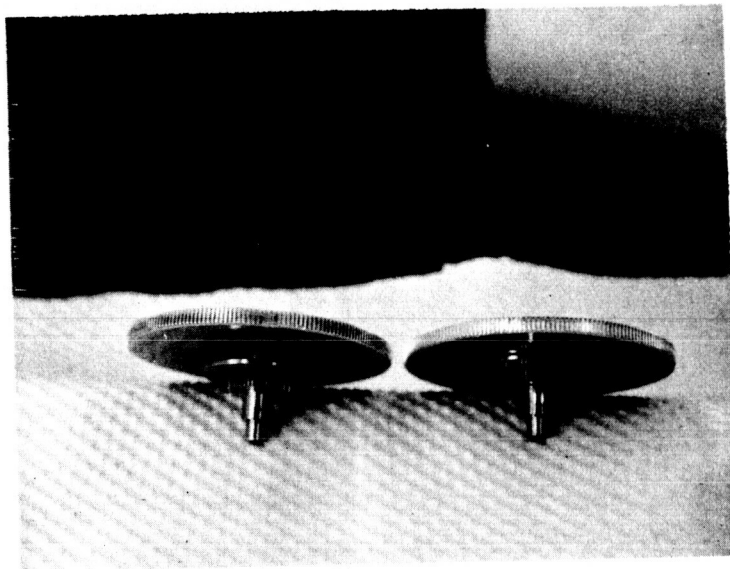


FIGURE 1

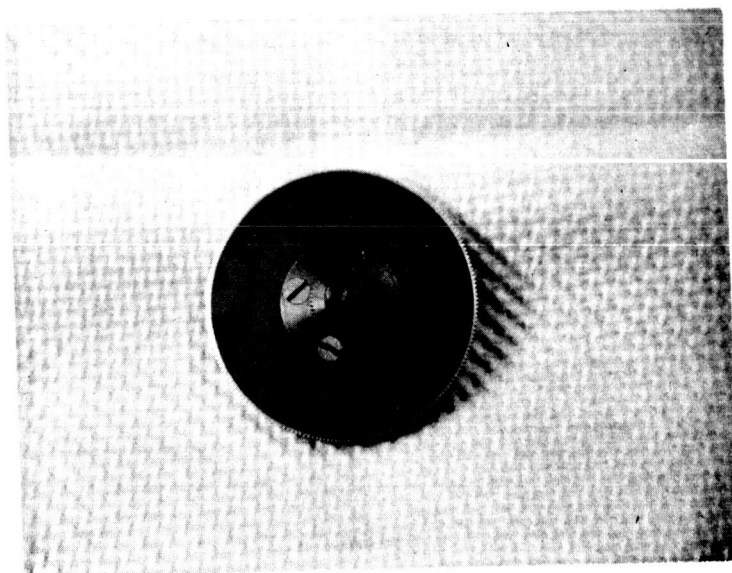


FIGURE 2

Remedial Action Taken:

None. The test was shorted and the unit returned to ITTIL for repairs.

No. of Previous Failures of this Nature: None

Can this failure be attributed to:

1. Design deficiency? possible
2. Workmanship?
3. Other (explain)?

Approved by:   
Title: Project Manager

Review Board

Review Held:                      Date 3/19/65

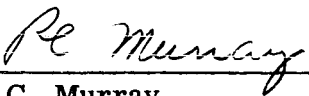
Conclusions:

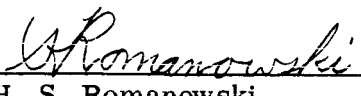
It was generally agreed that the interference fit between shaft and gear was insufficient to properly secure the gear during vibration. Agreement was not reached as to whether this was simply a defective assembly or an actual design deficiency.


Recommended Action:

It was recommended that the gear be permanently attached to the shaft flange in some manner. This was accomplished by drilling and tapping both to accept four #2-56 flat-head screws as shown in Figure 2.

Reviewed by:

  
\_\_\_\_\_  
P. C. Murray  
Electronic Engineer

  
\_\_\_\_\_  
H. S. Romanowski  
Mechanical Engineer

  
\_\_\_\_\_  
P. R. Sargent  
Mechanical Engineer

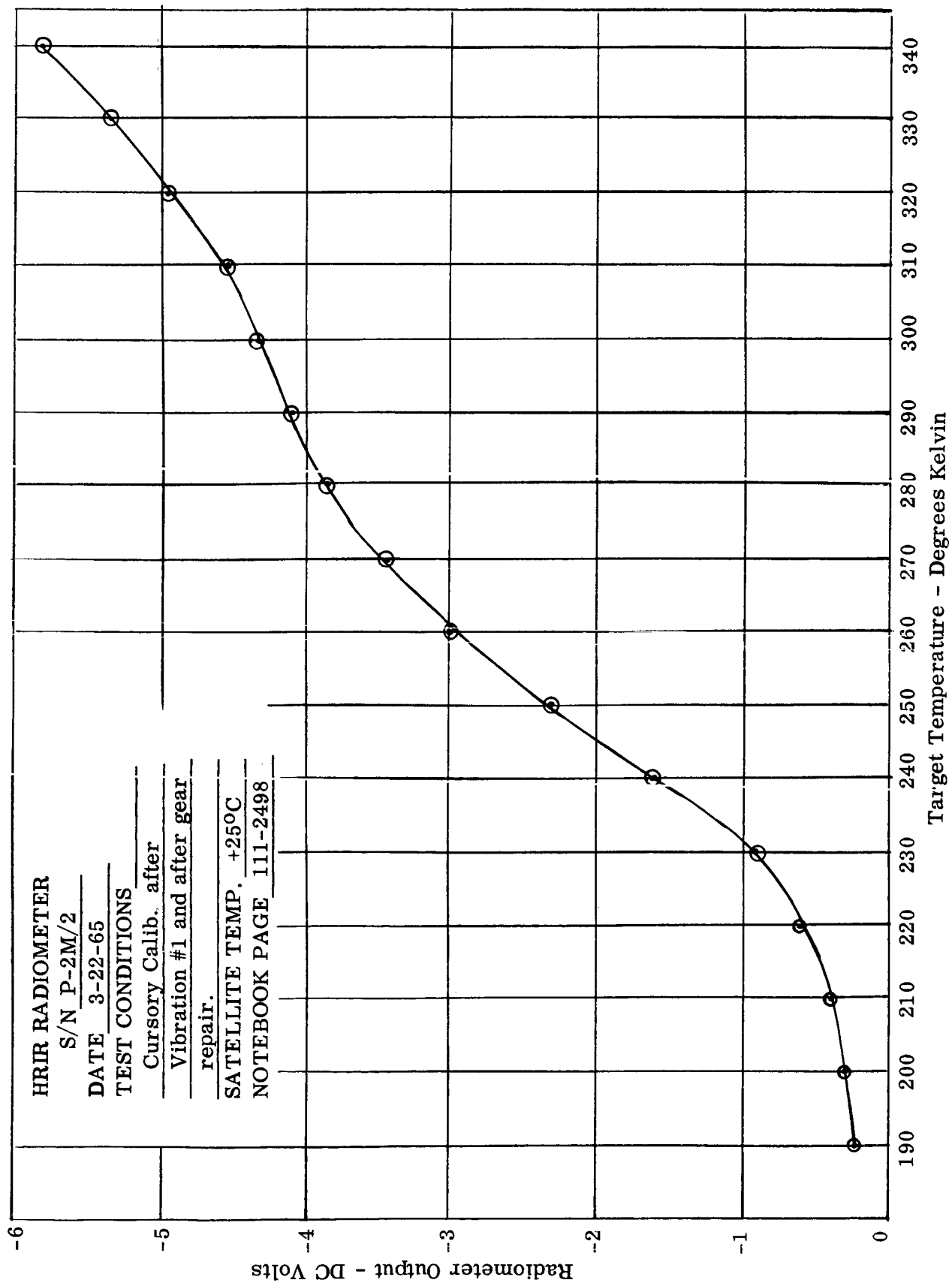
  
\_\_\_\_\_  
W. H. Wallschlaeger  
Project Manager

# Nimbus HRIR Radiometer Calibration

Date 3-22-65  
Page 1 of 1

Type of Calibration: Initial \_\_\_\_\_ Final \_\_\_\_\_ Check \_\_\_\_\_ After Vibration #1 \_\_\_\_\_  
Satellite Temperature +25 °C Pressure 2 x 10<sup>-6</sup> mm-hg  
Data Booklet No. --- HRIR Model and S/N P-2M/2

Target (°K)	190	200	210	220	230	240	250	260	270	280	290	300	310	320	330	340
Target (°C)																
Supply Voltage	24.6															
Supply Current	135															
-20 F/T TM	5.32															
-20 Reg. TM	4.92															
Ref A TM	3.92															
Temp. (°C)																
Ref B TM	4.04															
Ref E TM	3.32															
AGC TM	2.70															
Cell TM	2.11															
Temp. (-°C)																
Marker Ampl.																
No. Pulses																
Marker TM	4.05															
Motor TM	2.92															
Target Signal	0.25	0.30	0.40	0.60	0.90	1.60	2.30	3.00	3.45	3.85	4.10	4.35	4.55	4.95	5.35	5.80

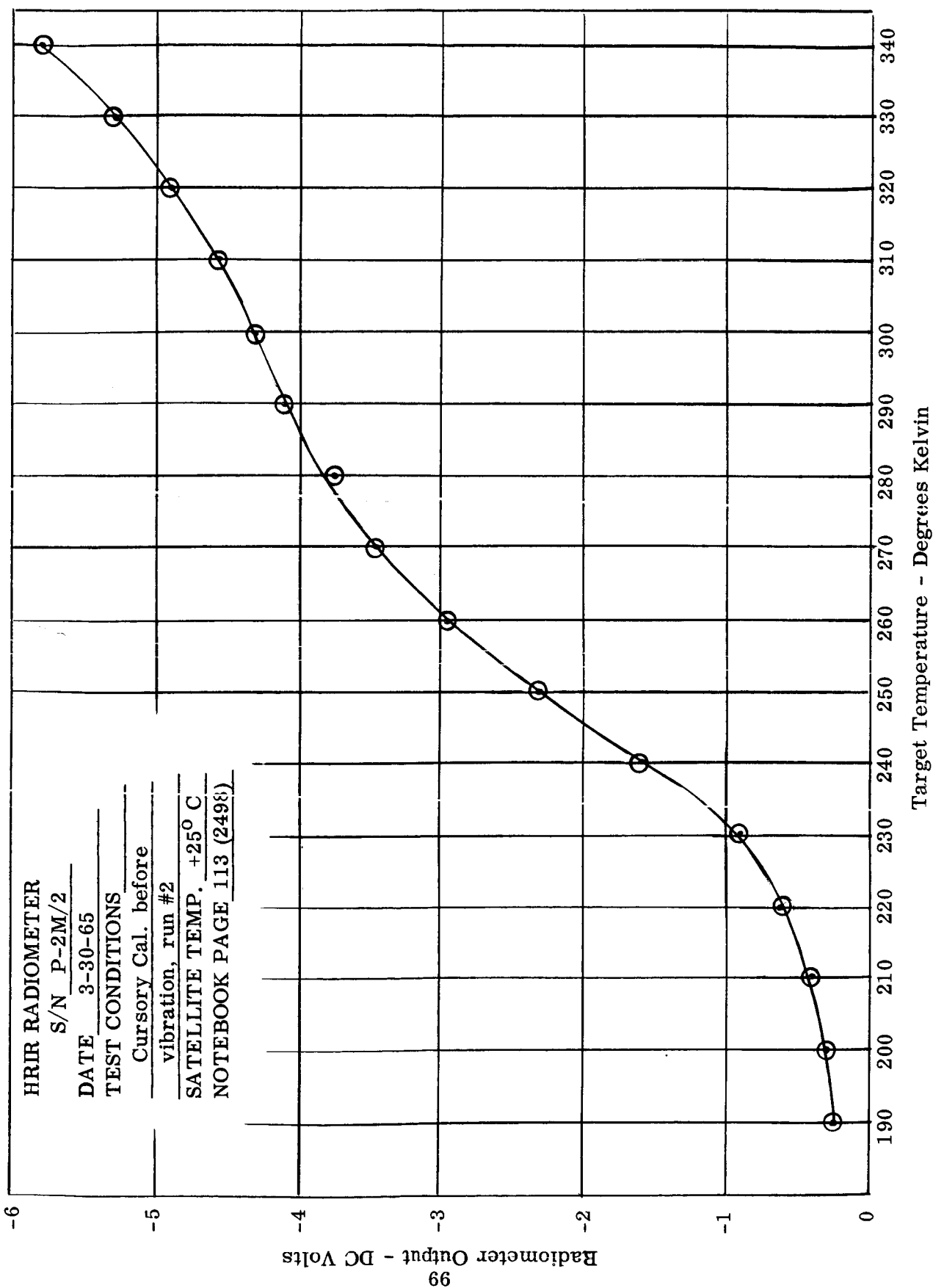


# Nimbus HRIR Radiometer Calibration

Date 3-30-65  
 Page 1 of 1

Type of Calibration: Initial \_\_\_\_\_ Final \_\_\_\_\_ Check \_\_\_\_\_ (Before #2 Vibration)  
 Satellite Temperature +25 °C Pressure 1.2 x 10<sup>-6</sup> mm-hg  
 Data Booklet No. --- HRIR Model and S/N \_\_\_\_\_ Proto. (P-2M/2)

Target (°K)	190	200	210	220	230	240	250	260	270	280	290	300	310	320	330	240
Target (°C)	-83	-73	-63	-53	-43	-33	-23	-13	-3	+7	+17	+27	+37	+47	+57	+67
Supply Voltage	24.6															24.6
Supply Current	131															136
-20 F/T TM	5.33															5.32
-20 Reg. TM	4.91															4.91
Ref A TM	3.76															3.59
Temp. (°C)	16.2															18.0
Ref B TM	3.87															3.68
Ref E TM	3.26															3.19
AGC TM	2.69															2.75
Cell TM	2.18															2.10
Temp. (-°C)	-78.5															77.9
Marker Ampl.	5.9															5.9
No. Pulses	7															7
Marker TM	4.05															4.05
Motor TM	2.97															2.89
Target Signal	0.25	0.30	0.40	0.60	0.90	1.60	2.30	2.95	3.45	3.75	4.10	4.30	4.55	4.90	5.30	580





## TEST REPORT

### NIMBUS HRIR RADIOMETER - NASA

Contract No. NAS 5-668

Model and Serial No: Pre-Prototype (P-2/M2)  
Test Environment: Sinusoidal Vibration  
Date of Test: April 2, 1965 Test Run No. 2  
Tested by: NASA-GSFC (T & E Branch)  
Equipment Used: MB-C125 Electronic Shaker System  
Method of Test: Cycle from 0-2000 cps at 0.25 SA, three planes 10g-peak  
(15 g-peak, 0-200 cps thrust axis) 2 octaves per minute.  
Specification: "An Environmental Specification for Nimbus Subsystems"  
Reference Log Sheet Nos: See failure report attached.  
Significant Results:

The unit was tested in the lateral transverse and longitudinal transverse axes with no failures. Due to a gear failure during longitudinal random vibration, no test was performed in the thrust axis.

The unit had previously undergone a resonance survey at 2g input levels in all three planes.

P. C. Murray  
P. C. Murray  
Responsible Test Engineer

W. H. Wallschlaeger  
W. H. Wallschlaeger  
Project Manager

## TEST REPORT

### NIMBUS HRIR RADIOMETER - NASA

Contract No. NAS 5-668

Model and Serial No: Pre-Prototypes (P-2/M2)  
Test Environment: Random Vibration  
Date of Test: April 2, 1965 Test Run No. 1  
Tested by: NASA-GSFC (T & E Branch)  
Equipment Used: MC-C125 Electronic Shaker System

Method of Test: Vibrate in each of three planes, 4 min, per plane with  
white noise 20-2000 cps; PSD = 0.2 g<sup>2</sup>/cps; 20 g-rms

Specification: "An Environmental Specification for Nimbus Subsystems"

Reference Log Sheet Nos: See Failure Report attached

#### Significant Results:

The unit was tested without incident in the lateral transverse axis. After 25 seconds of vibration in the longitudinal transverse axis, the mirror stopped turning and the test was halted.

The mirror seemed to be blocked at a point 90 degrees from nadir in the direction of the cooling cone opening. It appeared that the mirror magnetic pickup was hitting the gear slug at that point. The motor cover was removed and the pickup was checked and found to be secure and well locked.

The motor mount was removed to reveal the gear train. An examination revealed that the mirror drive gear had slipped on its shaft away from the shaft collar.

After appropriate repairs at ITTIL (see failure report) a cursory calibration confirmed that no change in calibration had taken place during vibration.

P. C. Murray  
P. C. Murray  
Responsible Test Engineer

W. H. Wallschlaeger  
W. H. Wallschlaeger  
Project Manager

## FAILURE REPORT

Date April 2, 1965 Time of failure Uncertain  
Project No. 11-20752 Other Reference HRIR (Modified)  
Contracting Agency NASA-GSFC Contract No. NAS 5-3683  
ITTIL Dept. No. 6130 Project Manager W. Wallschlaeger

Type of Failure: (Check Two)      Component X      Mechanical X  
   Subsystem \_\_\_\_\_      Electrical \_\_\_\_\_  
   System \_\_\_\_\_      Optical \_\_\_\_\_  
   Other \_\_\_\_\_      Other \_\_\_\_\_

Specify: Model or Part No. 4708139 Serial No. None

### Test Conditions at Time of Failure:

The unit was undergoing random vibration at 20 g-rms, 0.2 g<sup>2</sup>/cps, 20-2000 cps. Failure occurred after 25 seconds in this plane. (Longitudinal transverse)

### Nature of Failure:

The mirror stopped rotating at a point 90 degrees from nadir in the direction of the cooling cone opening. It appeared that the mirror magnetic pickup was hitting the gear slug at that point.

### Cause of Failure (if known):

The failure was caused by longitudinal separation of the gear from its shaft flange. This separation caused it to engage the mirror pickup, stopping at that point.

Remedial Action Taken:

None. The test was shorted, and the unit returned to ITTIL for repairs.

No. of Previous Failures of this nature: One (on the idler gear).

Can this failure be attributed to:

1. Design deficiency? X
2. Workmanship?
3. Other (explain)?

Approved by: *JH Walls Jr*  
Title: Project Manager

Review Board

Review Held:      Date: April 15, 1965

Conclusions:

It was generally agreed that the present design using a number 6 press fit for gear attachment was inadequate. A discussion brought out a number of various "fixes" that could be instituted on these and all future gear assemblies. The accepted methods for attaching gears on the three assemblies are illustrated in figure 1, 2 and 3.

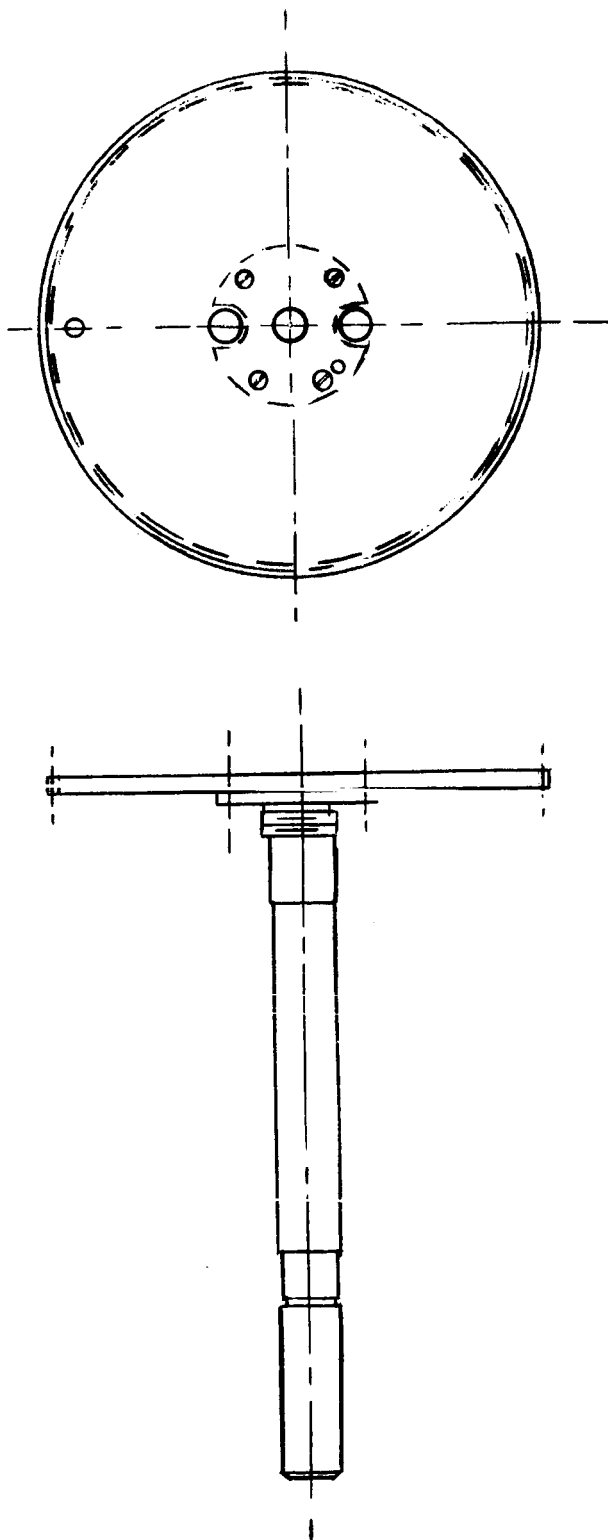


Figure 1 Scan Gear Assembly

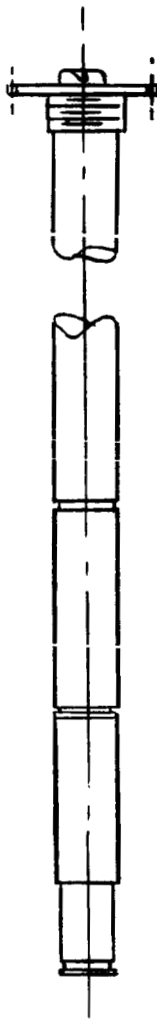
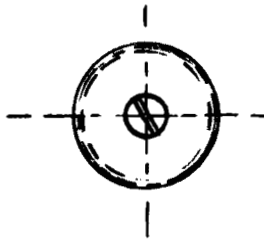


Figure 2 Chopper Gear Assembly

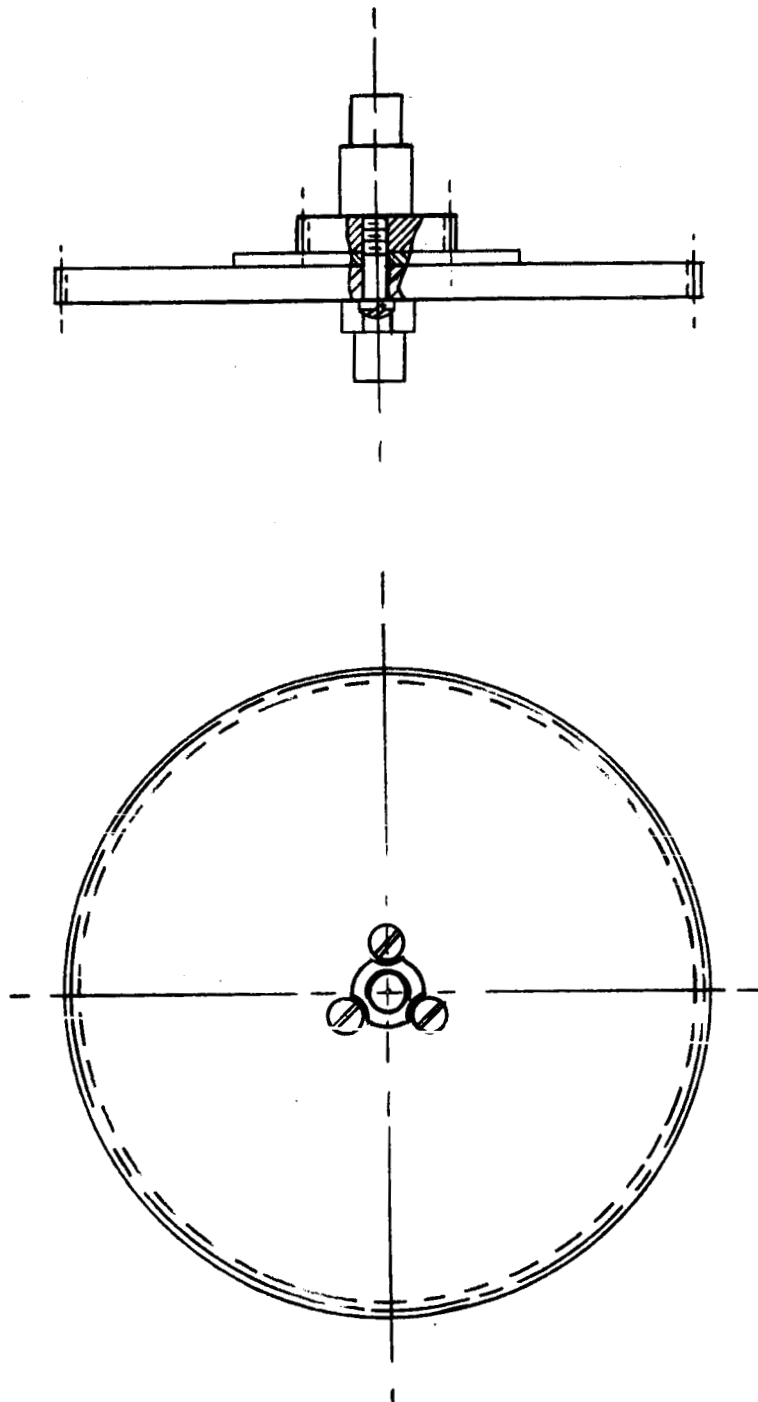


Figure 3 Idler Gear Assembly

Page Three

Recommended Action:

It was recommended that immediate action be taken to implement the agreed upon "fixes" in a new set of gear assemblies.

Reviewed by:

A. Arman, NASA-GSFC  
W. Burton, NASA-GSFC  
C. Catoe, NASA-GSFC  
C. Thienel, NASA-GSFC  
K. DeBrosse, ITTIL  
P. Murray, ITTIL  
H. Romanowski, ITTIL  
P. Sargent, ITTIL  
W. Wallschlaeger, ITTIL



# Nimbus HRIR Radiometer Calibration

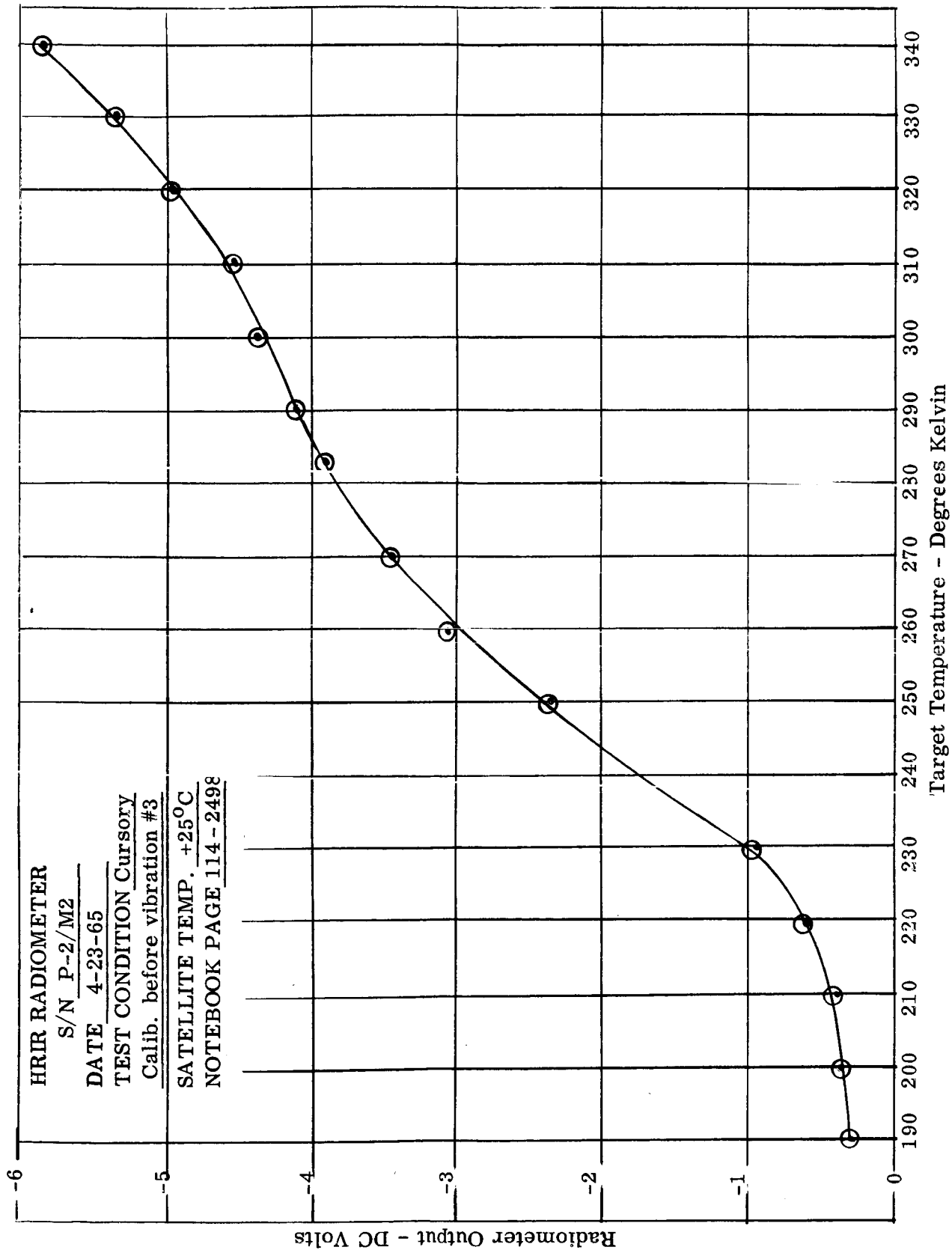
Cell reached Started Cooling  
-2.19 at 2200 at 1530  
6-1/2 hrs

Date 4-23-65  
Page 1 of 1

Type of Calibration: Initial Final Check Before Vibration #2  
Satellite Temperature +25 °C Pressure mm-hg  
Data Booklet No. --- HRIR Model and S/N P2/M2

Calib Sig = 6.0 V  
Cell On - 2.23 V  
Cell Off - 2.13 V

Target (°K)	190	200	210	220	230	240	250	260	270	280	290	300	310	320	330	340
Target (°C)	-83	-73	-63	-53	-43	-33	-23	-13	-3	+7	+17	+27	+37	+47	+57	+67
Supply Voltage	24.6															24.6
Supply Current	130															132
-20 F/T TM	5.33															5.32
-20 Reg. TM	4.91															4.91
Ref A TM	4.00															3.81
Temp. (°C)	+14															15.7
Ref B TM	4.11															3.91
Ref E TM	3.43															3.37
AGC TM	2.71															2.75
Cell TM	2.04															2.19
Temp. (-°C)	77.4															78.6
Marker Ampl.	5.75															
No. Pulses	7															7
Marker TM	4.05															4.05
Motor TM	2.99															3.08
Target Signal	0.30	0.35	0.40	0.60	0.95	1.75	2.35	3.05	3.45	3.90	4.10	4.35	4.55	4.95	5.35	5.85



On April 30, a calibration at +25 degrees C was made. (See pages 80 and 81 .) At this time it was apparent that a definite phasing shift had taken place such that at satellite temperatures above +25 degrees C, the lower temperature calibration points would be adversely affected. This apparently was due to a slight movement of the chopper pickup during vibration. This condition was reported to the NASA Technical Officer, and at his request, the pickup was rephased, and the unit given a full five-temperature calibration.

#### 4.5 Acceleration

Following vibration, an acceleration test was performed on the Genisco centrifuge at GSFC. The unit was mounted such that g-forces would be 30-g at an assumed CG of 2-1/2 inches above the mounting surface. The motor was energized during the test and the motor telemetering point was monitored. As centrifugal speed increased, the motor TM increased to a point indicating a stall condition. This condition prevailed during the entire 5 minute test until the centrifuge came to a stop, at which point the motor TM returned to a normal reading. All TM points read normal after the test. The test report is shown on page 82.

#### 4.6 Radiometric Calibrations

For calibration purposes, the radiometer was mounted in a vacuum chamber and the chamber evacuated to less than  $10^{-5}$  mm. hg. The radiometer mount was varied from 0 degree C to +50 degrees C in five steps (0 degree, +5 degrees, +25 degrees, +45 degrees, and +50 degrees C.) and the target cycled from 190 degrees K to 340 degrees K. Readings were taken on a Honeywell Visicorder in 10 degrees K steps throughout this range, at each mount temperature. The work sheets and calibrations curves are shown on pages 83 through 88. The actual visicorder tracings are reproduced in Appendix III (Volume II).

## TEST REPORT

### NIMBUS HRIR RADIOMETER - NASA Contract No. NAS 5-668

Model and Serial No: Pre-Prototype (P-2/M2)  
Test Environment: Sinusoidal Vibration  
Date of Test: April 28, 1965 Test Run No. 3  
Tested by: NASA-GSFC (T & E Branch)  
Equipment Used: MB-C125 Electronic Shaker System  
Method of Test: Cycle from 0-2000 cps at 0.25" SA. Three planes, 10g-pk  
(15g-pk, 0-200 cps thrust axis) 1 octave per minute.  
Specification: "An Environmental Specification for Nimbus Subsystems"  
Reference Log Sheet Nos: \_\_\_\_\_  
Significant Results:

The unit was tested in the thrust axis without incident.


After the lateral transverse axis test it was noted that the set screw used for mounting the scan mirror to its shaft was loose. This screw was retightened and testing resumed.


During the longitudinal transverse axis the mirror stopped rotating at 145 cps. The test was halted and the failure investigated. It was found that the relay mirror aperture had come loose, causing the chopper to jam. The aperture was removed and the unit reassembled. Since loc-tite was not immediately available, it was decided to resume the test without loc-tite on the mounting screws. The lateral axis test was repeated in its entirety without further incident.

It must be noted here that the relay aperture which failed has been proven superfluous and as such will be left out of the unit. Upon return to ITTIL all screws which were removed were treated with "yellow" loc-tite, including the scan mirror set-screw.

A calibration test at ITTIL at +25 degrees C indicated a definite phasing shift such that at satellite temperature above 25 degrees C, the low temperature calibration points would be adversely affected. This apparently was due to a slight movement of the chopper pickup during vibration.

This pickup will be rephased and a complete calibration performed at five satellite temperatures.

  
P. C. Murray  
Responsible Test Engineer

  
W. H. Walkschlaeger  
Project Manager


## TEST REPORT

### NIMBUS HRIR RADIOMETER - NASA

Contract No. NAS 5-668

Model and Serial No: Pre-Prototype (P-2/M2)  
Test Environment: Random Vibration  
Date of Test: April 28, 1965 Test Run No. 2  
Tested by: NASA-GSFC (T & E Branch)  
Equipment Used: MB-C125 Electronic Shaker System  
Method of Test: Vibrate in each of three planes 4 min/plane with white noise  
20-2000 cps; PSD = 0.2 g<sup>2</sup>/cps; 20 g-rms  
Specification: "An Environmental Specification for Nimbus Subsystem"  
Reference Log Sheet Nos: \_\_\_\_\_  
Significant Results:

The unit was tested in the thrust plane without any visible failure. After longitudinal vibration, the set-screw used to hold the scan mirror to its shaft was found to be loose. This screw was tightened and testing resumed. The lateral test was run with no evidence of failure. All telemetry points were checked and found to be normal. (See test report for April 28 Sinusoidal vibration for further comments on tests at ITTIL.)

  
P. C. Murray  
Responsible Test Engineer

  
W. H. Wallschlaeger  
Project Manager

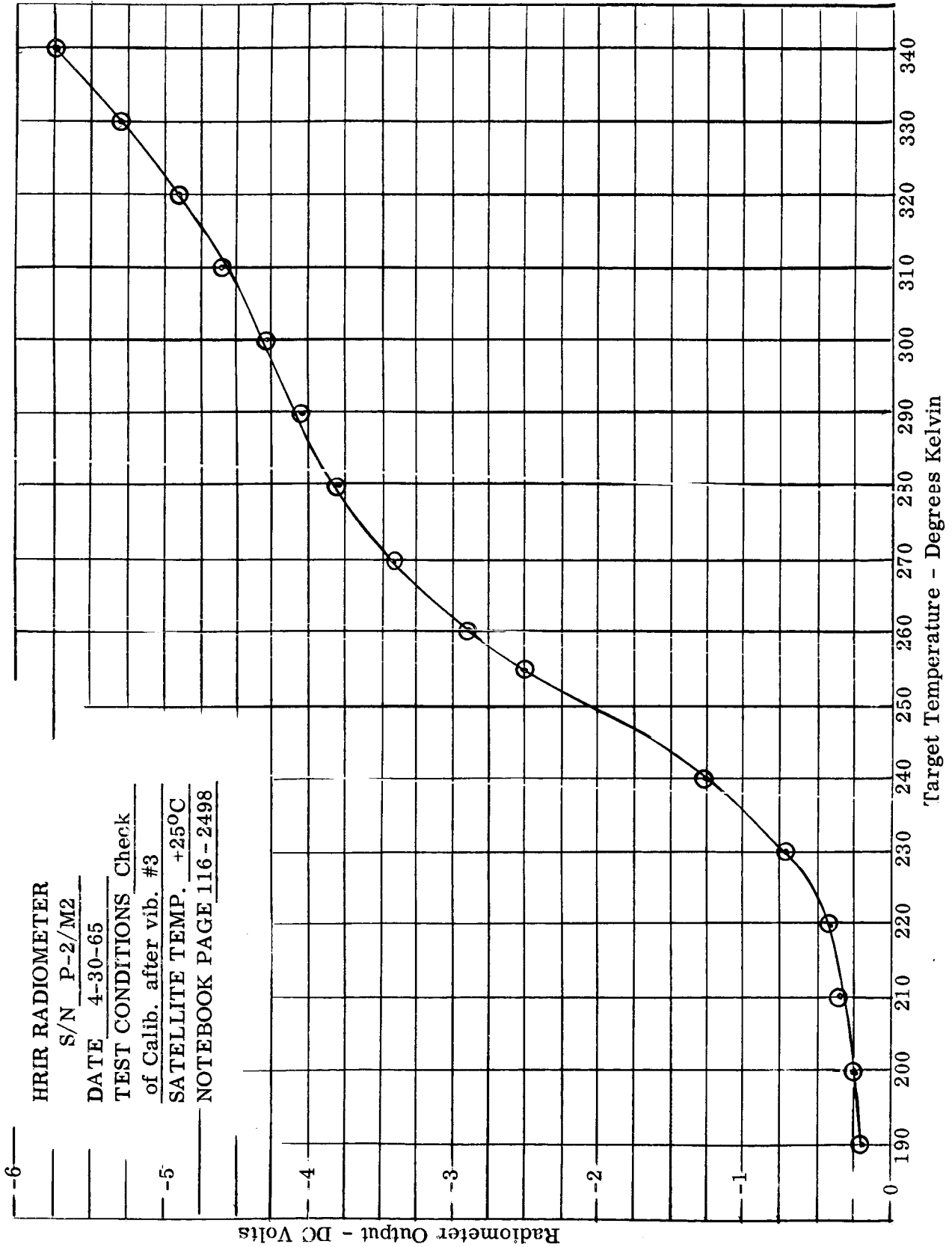
# Nimbus HRIR Radiometer Calibration

Date 4-30-65  
 Page 1 of 1

Type of Calibration: Initial Final Check (After Vibration #3)  
 Satellite Temperature +25 °C Pressure 2.4 x 10<sup>-6</sup> mm-hg  
 Data Booklet No. DB-P2/M2 HRIR Model and S/N P-2/M2

Calib. Signal = 5.95  
 Cell On - 2.23 V  
 Cell Off - 2.13 V

Target (°K)	190	200	210	220	230	240	250	260	270	280	290	300	310	320	330	340
Target (°C)	-83	-73	-63	-53	-43	-33	-23	-13	-3	+7	+17	+27	+37	+47	+57	+67
Supply Voltage	24.6															24.6
Supply Current	132															130
-20 F/T TM	5.32															5.32
-20 Reg. TM	4.92															4.91
Ref A TM	3.86															3.70
Temp. (°C)	15.5															17.0
Ref B TM	3.96															3.79
Ref E TM	3.24															3.18
AGC TM	2.72															2.78
Cell TM	2.16															2.14
Temp. (-°C)	78.4															78.2
Marker Ampl.	5.75															5.75
No. Pulses	7															7
Marker TM	4.05															4.05
Motor TM	3.03															2.98
Target Signal	0.20	0.25	0.35	0.40	0.70	1.25	2.50	2.90	3.40	3.80	4.05	4.30	4.60	4.90	5.30	5.75



## TEST REPORT

### NIMBUS HRIR RADIOMETER - NASA

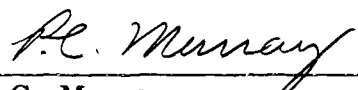
Contract No. NAS 5-668

Model and Serial No: Pre-Prototype (P-2/M2)  
Test Environment: Acceleration  
Date of Test: April 28, 1965 Test Run No: 1  
Tested by: NASA-GSFC (T & E Branch)  
Equipment Used: Genisco Centrifuge  
Method of Test: Static acceleration in thrust axis of 30g for five minutes  
continuous. Operation as in powered flight.  
Specification: "An Environmental Specification for Nimbus Subsystems"  
Reference Log Sheet Nos: \_\_\_\_\_  
Significant Results:

The unit was mounted on the centrifuge such that g-forces would be 30g at an assumed CG of 2-1/2 inches above the radiometer mounting surface. The motor was energized during the test and the Motor Telemetry was monitored.

As speed increased, the motor TM increased to a point indicating a stalled condition. This condition remained during the entire test until the centrifuge came to a stop, at which point the motor TM returned to its normal reading. All TM readings were normal after testing.

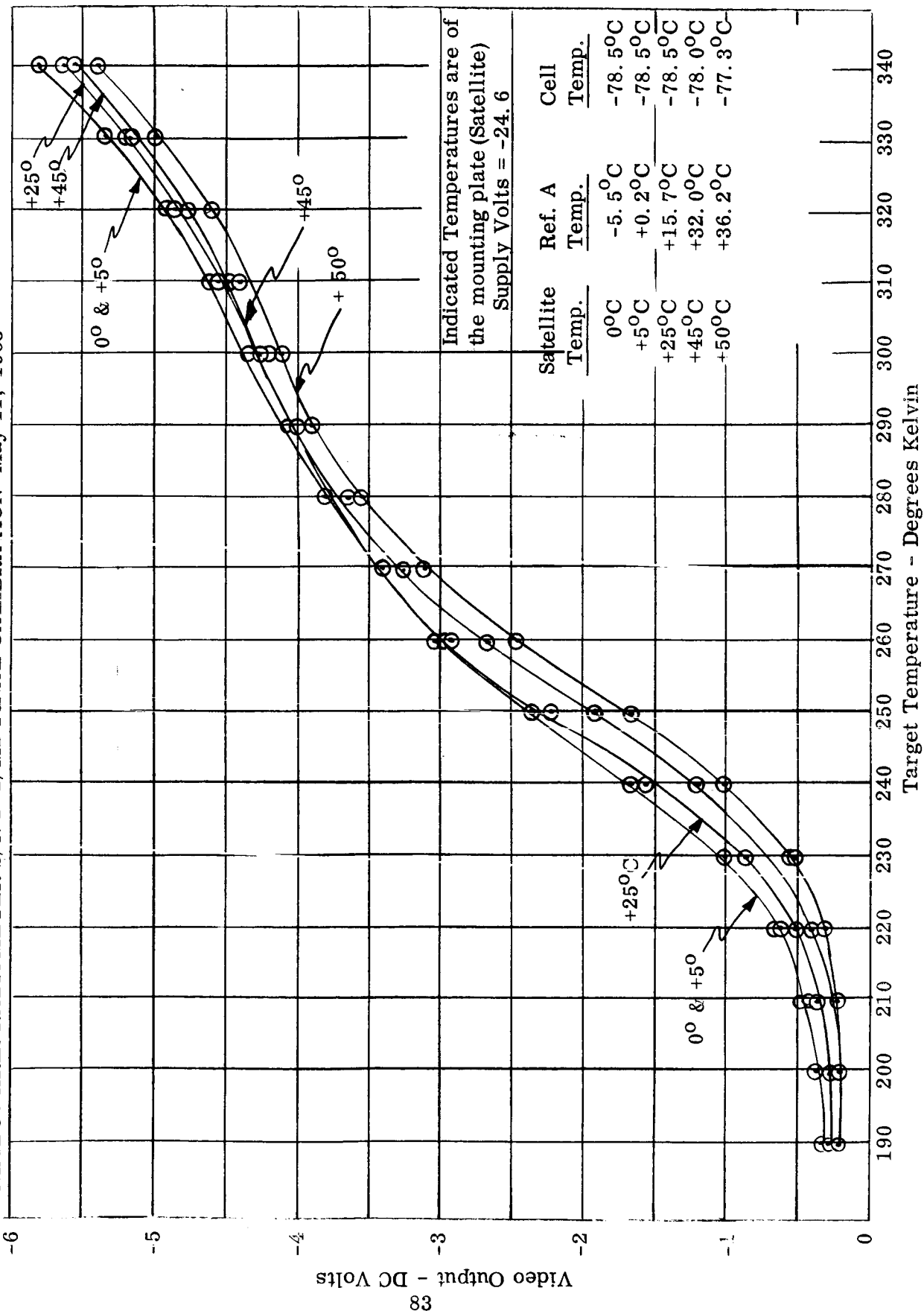
Based on the tests and results indicated above, it is recommended that this report be accepted as a valid prototype qualification test under static acceleration conditions.

  
\_\_\_\_\_  
P. C. Murray  
Responsible Test Engineer

  
\_\_\_\_\_  
W. H. Wallschlaeger  
Project Manager



# NIMBUS HRIR RADIOMETER S/N P-2/M2 FINAL CALIBRATION May 11, 1965



# Nimbus HRIR Radiometer Calibration

Date 5-5-65

Page 1 of 5

Type of Calibration: Initial      Final ×      Check  
 Satellite Temperature +25 °C      Pressure 2.4 x 10<sup>-6</sup> mm-hg  
 Data Booklet No. ---      HRIR Model and S/N P-2/M2

Calib Voltage = 5.95 V

Target (°K)	190	200	210	220	230	240	250	260	270	280	290	300	310	320	330	340
Target (°C)	-83	-73	-63	-53	-43	-33	-23	-13	-3	+7	+17	+27	+37	+47	+57	+67
Supply Voltage	24.6															24.6
Supply Current	130															130
-20 F/T TM	5.32															5.33
-20 Reg. TM	4.91															4.92
Ref A TM	3.81															3.65
Temp. (°C)	15.7															17.5
Ref B TM	3.91															3.74
Ref E TM	3.36															3.26
AGC TM	2.75															2.82
Cell TM	2.16															2.14
Temp. (-°C)	78.4															78.2
Marker Ampl.	5.7															5.65
No. Pulses	7															7
Marker TM	4.05															4.05
Motor TM	2.96															2.98
Target Signal	0.25	0.25	0.35	0.50	0.35	1.55	2.20	2.90	3.40	3.80	4.05	5.25	4.55	4.85	5.20	5.65

# Nimbus HRIR Radiometer Calibration

Date 5-6-65  
Page 2 of 5

Type of Calibration: Initial      Final      x      Check  
Satellite Temperature +50 °C      Pressure 1 x 10<sup>-6</sup> mm-hg  
Data Booklet No. ---      HRIR Model and S/N P-2/M2

Calib. Voltage = 5.85

Target (°K)	140	200	210	220	230	240	250	260	270	280	290	300	310	320	330	340
Target (°C)	-83	-73	-63	-53	-43	-33	-23	-13	-3	+7	+17	+27	+37	+47	+57	+67
Supply Voltage	24.6															24.6
Supply Current	128															128
-20 F/T TM	5.38															5.39
-20 Reg. TM	4.92															4.92
Ref A TM	2.17															2.08
Temp. (°C)	36.2															37.5
Ref B TM	2.25															2.15
Ref E TM	2.93															2.81
AGC TM	2.10															2.24
Cell TM	2.02															2.02
Temp. (-°C)	77.3															77.3
Marker Ampl.	5.65															5.70
No. Pulses	7															7
Marker TM	4.10															4.10
Motor TM	2.73															2.71
Target Signal	0.20	0.20	0.20	0.30	0.50	1.00	1.65	2.45	3.10	3.55	3.90	4.10	4.40	4.60	5.00	5.40

# Nimbus HRIR Radiometer Calibration

Date 5-7-65  
 Page 3 of 5

Type of Calibration: Initial Final X Check  
 Satellite Temperature +45 °C Pressure 1 x 10<sup>-6</sup> mm-hg  
 Data Booklet No. HRIR Model and S/N P-2/M2

Calib. Voltage - 5.90 V

Target (°K)	190	200	210	220	230	240	250	260	270	280	290	300	310	320	330	340
Target (°C)	-83	-73	-63	-53	-43	-33	-23	-13	-3	+7	+17	+27	+37	+47	+57	+67
Supply Voltage	24.6															24.6
Supply Current	129															130
-20 F/T TM	5.37															5.37
-20 Reg. TM	4.92															4.92
Ref A TM	2.44															2.34
Temp. (°C)	32.0															33.5
Ref B TM	2.53															2.42
Ref E TM	3.03															2.91
AGC TM	2.25															2.35
Cell TM	2.12															2.12
Temp. (-°C)	78.0															78.0
Marker Ampl.	570															580
No. Pulses	7															7
Marker TM	4.10															4.05
Motor TM	2.78															2.87
Target Signal	0.20	0.20	0.20	0.40	0.55	1.20	1.90	2.65	3.25	3.65	4.00	4.25	4.45	4.75	5.15	5.55

# Nimbus HRIR Radiometer Calibration

Date 5-11-65  
 Page 4 of 5

Type of Calibration: Initial          Final          X          Check           
 Satellite Temperature 0 °C Pressure 3.6 x 10<sup>-6</sup> mm-hg  
 Data Booklet No.          HRIR Model and S/N P-2/M2

Cell On - 2.24 V (78.9°)  
 Cell Off - 2.14 V (78.2°)

Calib Volt. = 5.95 V

Target (°K)	190	200	210	220	230	240	250	260	270	280	290	300	310	320	330	340
Target (°C)	-83	-73	-63	-53	-43	-33	-23	-13	-3	+7	+17	+27	+37	+47	+57	+67
Supply Voltage	24.6															24.6
Supply Current	134															134
-20 F/T TM	5.27															5.27
-20 Reg. TM	4.91															4.90
Ref A TM	6.24															6.01
Temp. (°C)	-5.5															-3.5
Ref B TM	6.34															6.09
Ref E TM	3.51															3.48
AGC TM	3.24															3.35
Cell TM	2.10															2.16
Temp. (-°C)	78.6															78.4
Marker Ampl.	5.75															5.75
No. Pulses	7															7
Marker TM	4.05															4.05
Motor TM	3.26															3.24
Target Signal	0.30	0.35	0.40	0.60	1.00	1.65	2.35	3.00	3.40	3.80	4.00	4.35	4.60	4.90	5.35	5.80

# Nimbus HRIR Radiometer Calibration

Date 5-11-65  
 Page 5 of 5

Type of Calibration: Initial X Final X Check       
 Satellite Temperature +5 °C Pressure 3.2 x 10<sup>-6</sup> mm-hg  
 Data Booklet No.      HRIR Model and S/N P-2/M2  
 Cell On = 2.24 V  
 Cell Off = 2.14 V

	190	200	210	220	230	240	250	260	270	280	290	300	310	320	330	340
Target (°K)																
Target (°C)	-83	-73	-63	-53	-43	-33	-23	-13	-3	+7	+17	+27	+37	+47	+57	+67
Supply Voltage	24.6															24.6
Supply Current	133															133
-20 F/T TM	5.28															5.27
-20 Reg. TM	4.90															4.90
Ref A TM	5.55															5.39
Temp. (°C)	+0.2															+1.5
Ref B TM	5.64															5.47
Ref E TM	3.37															3.29
AGC TM	3.19															3.23
Cell TM	2.19															2.24
Temp. (-°C)	78.6															78.9
Marker Ampl.	5.75															5.65
No. Pulses	7															7
Marker TM	4.05															4.05
Motor TM	3.17															3.19
Target Signal	0.30	0.35	0.45	0.65	1.00	1.65	2.35	2.95	3.40	3.80	4.00	4.20	4.55	4.80	5.20	5.65

## 5.0 NEW TECHNOLOGY

Items developed under this contract which are considered new technology pursuant to the NASA New Technology clause of September 1964, are the epoxy cooling patch support rings, detector temperature control, and electronic offset.

### 5.1 Epoxy Cooling Patch Support Rings

Technology concerning the support rings is fully discussed in Section 3.2.

### 5.2 Detector Temperature Control

Covered in Section 2.4.

### 5.3 Electronic Offset

Covered in Section 2.2.